Elementary excitations of high-degree pair interactions: The two-spin–deviation spectra for a spin-1 ferromagnet*

S. T. Chiu-Tsao, Peter M. Levy, and C. Paulson
Department of Physics, New York University, 4 Washington Place, New York, New York 10003
(Received 9 December 1974)

We consider a ferromagnetic linear chain and a simple-cubic lattice of spin-1 ions with isotropic dipolar and quadrupolar pair interactions. We calculate the zero-temperature energy spectra of two-spin–deviation states over the entire range of β (the ratio of the quadrupolar to dipolar coupling), $-1 < \beta \leq 1$, for which the system has a ferromagnetic ground state. We also calculate the spectral density of states for "quadrupolar" excitations, which are single-ion two-spin–deviation excitations. We find that, in addition to the two-spin–wave bound states outside the band, there exists a new "quadrupolar" resonant state within the band, which is seen as a distinctive peak in the spectral density of states for quadrupolar excitations. The linewidth of the peak decreases and the peak moves to a lower position in the band as β increases. As β approaches 1 the quadrupolar resonant state becomes a "quadrupole wave" excitation, which is an eigenstate of the Hamiltonian and describes the coherent propagation of quadrupolar excitations in the solid. The dispersion relation of the quadrupole wave is the same as that of the spin wave. We also find that, when β is sufficiently negative, there is a repulsive interaction between two spin waves, which causes bound states to split off above the band. We show that both the dipolar and quadrupolar pair interactions can in principle be simultaneously determined from the Raman spectra of the isotropic system. Finally, we comment on the generalizations of the present calculations to more realistic cases.

I. INTRODUCTION

In recent years it has been shown that high-degree pair interactions between magnetic ions may be comparable or even stronger than the dipolar couplings, especially in rare-earth compounds.[1] Rare-earth ions retain many of their free-ion properties when they form solids. In particular, the total angular momentum $\vec{J}=\vec{L}+\vec{S}$ remains a relatively good quantum number. In a first approximation the effect of the crystalline surroundings on a rare-earth ion is to split the $(2J+1)$-fold degeneracy of the ground manifold. If the surrounding has high point group symmetry, e.g., cubic O_h symmetry, the split levels will still be degenerate; the orbital angular momentum of the rare-earth ion is not quenched. The existence of the degenerate levels means that high-degree pair interactions between rare-earth ions can be present. There are several mechanisms which contribute to such interactions,[1] e.g., electric multipole interactions, Jahn-Teller effects (virtual phonon coupling), multielectron exchange (Schrödinger's idea), and the contribution of orbital anisotropy to exchange interactions.

It is of interest to understand how the high-degree pair interactions affect the elementary excitation spectra in rare-earth compounds. Several studies have been made on this.[2–5] The purpose of this paper is to study the effects of *large* high-degree pair interactions on the two-spin-deviation states of a ferromagnet. We are particularly interested in showing how a new dynamical symmetry of the Hamiltonian manifests itself in the excitation spectrum. For this reason, we will consider a Hamiltonian which is rotationally invariant, although realistic Hamiltonians contain anisotropic pair interactions and single-ion anisotropy. We also restrict ourselves to the case of spin 1 because this is the simplest case for which high-degree terms are present.

The system we consider is described by the Hamiltonian

$$\mathcal{H}=\mathcal{H}^{(1)}+\mathcal{H}^{(2)}, \tag{1}$$

where

$$\mathcal{H}^{(l)}=-\sum_{-l\leq m\leq l}(-1)^m\Gamma^{(l)}\sum_{i,j}\mathcal{O}_m^l(i)\mathcal{O}_{-m}^l(j), \tag{2}$$

where $\Gamma^{(1)} > |\Gamma^{(2)}| \geq 0$ so that the exact ground state of the system is ferromagnetic.[6] The terms $\mathcal{H}^{(1)}$ and $\mathcal{H}^{(2)}$ represent, respectively, the dipolar and quadrupolar interactions. The summation is over nearest-neighbor pairs of ions. The operators $\mathcal{O}_m^l$ are spherical tensor operators defined by Judd.[7] $\mathcal{O}_m^l(i)$ is an abbreviation for $\mathcal{O}_m^l(s_i^x, s_i^y, s_i^z)$. Specifically, the $\mathcal{O}_m^l$ are related to spin operators in the following way for $s=1$:

$$\mathcal{O}_0^1=(1/\sqrt{2})\,s_z,\qquad \mathcal{O}_{\pm1}^1=\mp\tfrac{1}{2}s^{\pm}, \tag{3a}$$

and

$$\mathcal{O}_0^2=(1/\sqrt{6})(3s_z^2-2),\qquad \mathcal{O}_{\pm1}^2=\mp\tfrac{1}{2}(s_zs^{\pm}+s^{\pm}s_z),\qquad \mathcal{O}_{\pm2}^2=\tfrac{1}{2}(s^{\pm})^2. \tag{3b}$$

In terms of spin operators, the Hamiltonian $\mathcal{H}$, Eq. (1), can be written as

$$\mathcal{H} = -J\sum_{i,j} \vec{s}_i \cdot \vec{s}_j - K\sum_{i,j} (\vec{s}_i \cdot \vec{s}_j)^2 - \tfrac{4}{3}\Gamma^{(2)}, \qquad (4)$$

where

$$J = \tfrac{1}{2}(\Gamma^{(1)} + \Gamma^{(2)}),$$

$$K = \Gamma^{(2)}.$$

Pink and Tremblay[2] have studied the effect of isotropic quadrupolar interactions on the two-spin-wave bound state spectrum by locating the poles of the Green's functions for $s = 1, 2$ and for

$$|K/J| \leq 0.25. \qquad (5a)$$

From Eq. (4) we find that the range of K/J in Eq. (5a) is equivalent to

$$\tfrac{1}{7} \geq \beta \geq -\tfrac{1}{9} \text{ for } s = 1, \qquad (5b)$$

where

$$\beta \equiv \Gamma^{(2)}/\Gamma^{(1)}. \qquad (6)$$

They also considered the effect of single-ion anisotropy on the spectrum. Later Pink and Ballard[3] extended these calculations to the cases where the anisotropy of the pair interactions is included. In this paper, we are particularly interested in studying the case where *large* quadrupolar interactions are present, i.e., $|\beta|$ approaching 1.

We formulate our problem by constructing wave functions of the two-spin-deviation states based directly on the Schrödinger equation. We find that there is a single-ion resonant state within the band in addition to the bound states outside the band. As it requires a tensor operator of rank 2 or greater to excite the single-ion resonant state (in a one step process), we will call it a "quadrupolar" resonant state. This quadrupolar resonant state shows up as a distinctive peak in the spectral density of states for quadrupolar (single-ion two-spin-deviation) excitations which we also calculate in this paper. The line width of the peak decreases and the peak moves to a lower position in the band as β increases. At the zone center, such a density of states may be observed by Raman scattering. Mechanisms for these single-ion excitations have been derived by Moriya,[8] Elliott and Loudon,[9] and Thorpe.[10]

When $\beta = 1$, the Hamiltonian possesses a new dynamical symmetry, namely, SU(3) symmetry, in addition to SU(2) symmetry. Then the resonant state becomes an eigenstate of the Hamiltonian, called a "quadrupole wave," which is degenerate with the spin-wave excitation.[11] This excitation is gapless and is a new Goldstone mode of the system. The quadrupole wave describes the coherent propagation of two spin deviations on the same site through the lattice. This excitation is different from the single-ion bound states[3,12] for which two spin deviations are localized on the same site only at the zone boundary. For $\beta = 1$ the spectral density of states of quadrupolar excitations has a δ-function peak at the quadrupole-wave energy. The quadrupole wave and quadrupolar resonant states are the main results of this paper. We also study the exchange bound states outside the band and we extend Pink and Tremblay's calculation[2] to large values of $|\beta|$. We find that, when β is sufficiently negative, there is repulsive interaction between two spin waves, which causes bound states to split off above the band. In addition to obtaining the bound-state energies, we calculate the relative weights of the density of states associated with the bound states compared to that of the excitations in the band.

In Sec. II we present our formalism and derive the bound-state condition from the Schrödinger equation. In Sec. III we obtain the exact zero-temperature two-spin-deviation spectrum and behavior of the wave functions for $1 \geq \beta > -1$ for a linear chain and a simple-cubic lattice. In Sec. IV we calculate the spectral density of states for quadrupolar (single-ion two-spin-deviation) excitations. Finally in Sec. V, we discuss our results and comment on the generalization of the present calculations to more realistic cases. In Appendix A, we discuss the symmetry properties and the classification of the eigenstates of a general class of isotropic Hamiltonians of which the Hamiltonian in Eq. (1) is a special case. In Appendix B, we present a qualitative study of the effects on the two-spin-deviation spectra of the individual terms in a spin-1 Hamiltonian with pair anisotropy. In Appendix C, we discuss the symmetry of the bound-state wave functions for the simple-cubic lattice.

II. FORMALISM

We consider a ferromagnetic system of effective spin-1 ions described by the Hamiltonian, Eqs. (1) and (2). The symmetry properties and the classification of the eigenstates of this Hamiltonian are discussed in Appendix A. Both $\mathcal{H}^{(1)}$ and $\mathcal{H}^{(2)}$ in Eq. (2) and hence $\mathcal{H}$ in Eq. (1) are invariants of the SU(2) group. In addition, when $\beta = 1$, $\mathcal{H}$ is an invariant of the SU(3) group. The commutation relations are as follows:

For all values of β, we have

$$[S_\mu, \mathcal{H}] = 0$$

and

$$[S^2, \mathcal{H}] = 0, \qquad (7)$$

where

$$S_\mu \equiv \sum_i s_\mu(i) \quad (\mu = x, y, z)$$

and

$$S^2 = S_x^2 + S_y^2 + S_z^2 .$$

However, only for $\beta = 1$,

$$\left[\sum_i \mathcal{O}_m^2(i), \mathcal{H}\right] = 0 \tag{8}$$

where $-2 \leq m \leq 2$. Since $\mathcal{H}$ is rotationally invariant, we label the eigenstates of the Hamiltonian $\mathcal{H}$ by the z component of the total spin of the system S_z. Assuming that in the ferromagnetic ground state all the spins are aligned along the z direction, we have $S_z = N$, where N is the number of ions in the system. The excited states are characterized by the number of spin deviations, defined by

$$m \equiv N - S_z .$$

The one-spin-deviation ($m = 1$) states are spin waves. For completeness, we discuss them in Sec. II A. We will study the properties of the two-spin-deviation ($m = 2$) states in detail in Sec. II B.

A. Spin waves

The one-spin-deviation state can be written in the form

$$|\psi_1\rangle = \sum_i \phi(\vec{r}_i)\, s_i^-|g\rangle . \tag{9}$$

$\phi(\vec{r}_i)$ is the probability amplitude of creating a spin deviation at site i, s_i^- is the spin-lowering operator at site i acting on the ferromagnetic ground state $|g\rangle$. To determine $\phi(\vec{r}_i)$, we rewrite the Schrödinger equation

$$\mathcal{H}|\psi_1\rangle = E_1|\psi_1\rangle , \tag{10}$$

by using the spin commutation relations, in the form

$$(\Gamma^{(1)} + \Gamma^{(2)}) \sum_{\vec{\delta}} [\phi(\vec{r}_j) - \phi(\vec{r}_j + \vec{\delta})] = (E_1 - E_g)\,\phi(\vec{r}_j) , \tag{11}$$

where $\vec{\delta}$ is the vector connecting nearest neighbors, and E_g is the ground-state energy. Equation (11) can be easily solved. We obtain the wave function and energy of a simple spin wave of wave vector $\vec{k}$

$$\phi(\vec{r}_j) = e^{i\vec{k}\cdot\vec{r}_j} \tag{12}$$

and

$$E_1 = E_g + (\Gamma^{(1)} + \Gamma^{(2)})\left(z - \sum_{\vec{\delta}} \cos\vec{k}\cdot\vec{\delta}\right). \tag{13}$$

This result agrees with that by Nauciel-Bloch *et al.*[6] We write the spin wave state as

$$S^-(k)|g\rangle \equiv \frac{1}{\sqrt{N}} \sum_j e^{i\vec{k}\cdot\vec{r}_j} s_j^-|g\rangle . \tag{14}$$

Besides the decrease in S_z by 1 from the ferromagnetic state, the spin wave carries with it a change in the z component of the quadrupole moment

$$Q \equiv \sum_i [3s_z^2(i) - 2], \tag{15}$$

because

$$QS^-(k)|g\rangle = (N-3)S^-(k)|g\rangle \tag{16}$$

and

$$Q|g\rangle = N|g\rangle . \tag{17}$$

We note that the spin-wave excitation energy is proportional to the sum of $\Gamma^{(1)}$ and $\Gamma^{(2)}$. Unless $\Gamma^{(1)}$ is fixed by some other experimental data, one cannot identify the presence of quadrupolar interactions only from the measurement of spin-wave spectra. In the following, we will show that both $\Gamma^{(2)}$ and $\Gamma^{(1)}$ can be simultaneously determined from the energy spectra of two-spin-deviation states.

B. Two-spin-deviation states

The two-spin-deviation ($m = 2$) states consist of two-ion and single-ion excitations. We note that the z component of the quadrupole moment Q of the two-ion excitations is equal to $N - 6$, while that of the single-ion excitations is equal to N. Unless Q is a good quantum number of the system, the eigenstates of our Hamiltonians are combinations of both kinds of excitations and can be written in the form

$$|\psi_2\rangle = \sum_{i,j} \Phi(\vec{r}_i, \vec{r}_j)|i,j\rangle \equiv \sum_{i,j} \Phi(\vec{r}_i, \vec{r}_j)\, s_i^- s_j^-|g\rangle . \tag{18}$$

By using the spin commutation relations and the identity

$$\langle jj'|ii'\rangle = 4s^2(1 - \delta_{i,i'}/2s)(\delta_{i,j}\delta_{i',j'} + \delta_{i,j'}\delta_{i',j}), \tag{19}$$

we write the Schrödinger equation for two-spin-deviation states in the following form

$$2z\Gamma^{(1)}\phi(\vec{r}_j, \vec{r}_j) - 2\Gamma^{(2)} \sum_{\vec{\delta}} \phi(\vec{r}_j + \vec{\delta}, \vec{r}_j + \vec{\delta}) - 2(\Gamma^{(1)} - \Gamma^{(2)}) \sum_{\vec{\delta}} \phi(\vec{r}_j, \vec{r}_j + \vec{\delta}) = (E - E_g)\,\phi(\vec{r}_j, \vec{r}_j), \tag{20a}$$

and for $j \neq j'$

$$(\Gamma^{(1)} + \Gamma^{(2)})\left(2z\,\phi(\vec{r}_j, \vec{r}_{j'}) - \sum_{\vec{\delta}'} [\phi(\vec{r}_j + \vec{\delta}', \vec{r}_{j'}) + \phi(\vec{r}_j, \vec{r}_{j'} + \vec{\delta}')]\right) - \{(\Gamma^{(1)} + 3\Gamma^{(2)})\,\phi(\vec{r}_j, \vec{r}_{j'}) - 2\Gamma^{(2)}[\phi(\vec{r}_{j'}, \vec{r}_{j'})$$

$$+ \phi(\vec{r}_j, \vec{r}_j)]\}\,\delta(\vec{r}_j, \vec{r}_{j'} + \vec{\delta}) = (E - E_g)\phi(\vec{r}_j, \vec{r}_{j'}), \tag{20b}$$

where $\phi(\vec{r}_i, \vec{r}_j) = [1 - (1/2s)\delta_{ij}]\Phi(\vec{r}_i, \vec{r}_j)$. Since the system is translationally invariant, we introduce the Fourier transform of $\phi(\vec{r}_j, \vec{r}_{j'})$:

$$\phi(\vec{r}_j, \vec{r}_{j'}) = \sum_{\vec{K}} e^{i\vec{K}\cdot(\vec{r}_j + \vec{r}_{j'})/2} \varphi_{\vec{K}}(\vec{r}_j - \vec{r}_{j'}) . \tag{21}$$

By substituting Eq. (21) into Eqs. (20), we obtain a set of N equations in the form:

$$(\mathcal{H}_0 + \tilde{V})\varphi_{\vec{K}}(\vec{R}) = (E - E_g)\varphi_{\vec{K}}(\vec{R}) , \tag{22}$$

where

$$\vec{R} \equiv \vec{r}_j - \vec{r}_{j'} , \tag{22a}$$

$$\mathcal{H}_0 \varphi_{\vec{K}}(\vec{R}) = 2(\Gamma^{(1)} + \Gamma^{(2)}) \times \left[z\varphi_{\vec{K}}(\vec{R}) - \sum_{\vec{\delta}} \cos\left(\frac{\vec{K}\cdot\vec{\delta}}{2}\right)\varphi_{\vec{K}}(\vec{R} + \vec{\delta}) \right] ,$$

$$\tilde{V}\varphi_{\vec{K}}(\vec{R}) = -\Gamma^{(1)} \left[\delta(\vec{R}, \vec{\delta}) f(\vec{\delta}) \right. \tag{22b}$$

$$\left. - \delta(\vec{R}, 0) \sum_{\vec{\delta}'} \cos\left(\frac{\vec{K}\cdot\vec{\delta}'}{2}\right) f(\vec{\delta}') \right] , \tag{22c}$$

where

$$f(\vec{R}) = (1 + 3\beta)\varphi_{\vec{K}}(\vec{R}) - 4\beta \cos\left(\frac{\vec{K}\cdot\vec{R}}{2}\right)\varphi_{\vec{K}}(0) . \tag{22d}$$

The term $\tilde{V}\varphi_{\vec{K}}(\vec{R})$ is the manifestation of the interaction between a pair of spin waves. In the absence of the term $\tilde{V}\varphi_{\vec{K}}(\vec{R})$ Eq. (22) describes two free spin waves with total wave vector $\vec{K}$ and excitation energy $\mathcal{E} \equiv E - E_g$

$$\mathcal{E}(\vec{K}, \vec{k}) = 2\Gamma^{(1)}(1 + \beta) \times \left[z - \sum_{\vec{\delta}} \cos\left(\frac{\vec{K}\cdot\vec{\delta}}{2}\right)\cos(\vec{k}\cdot\vec{\delta}) \right] , \tag{23a}$$

and wave function

$$\varphi_{\vec{K},\vec{k}}(\vec{R}) \propto \cos(\vec{k}\cdot\vec{R}) , \tag{23b}$$

where $2\vec{k}$ is the relative wave vector of the pair. By using Eqs. (22) we can derive the expression for the scattering potential between two spin waves in terms of the total and relative wave vectors.

$$V(\vec{K}, \vec{k}_1, \vec{k}_2) = -\Gamma^{(1)} \sum_{\vec{\delta}} \left[(1 + 3\beta)\cos(\vec{k}_2\cdot\vec{\delta}) - 4\beta \right. \times \cos\left(\frac{\vec{K}\cdot\vec{\delta}}{2}\right) \left. \left[\cos(\vec{k}_1\cdot\vec{\delta}) - \cos\left(\frac{\vec{K}\cdot\vec{\delta}}{2}\right) \right] \right] , \tag{24}$$

where $2\vec{k}_1$, $2\vec{k}_2$ are, respectively, the incoming and outgoing relative wave vectors of the two interacting spin waves. In the special case that $\beta = 0$, the Heisenberg case, this expression agrees with that given by previous authors.[13] We note that V can be attractive or repulsive, depending on the values of β, $\vec{K}$, $\vec{k}_1$, and $\vec{k}_2$.

The solution of Eq. (22) at the zone boundary where $\cos(\vec{K}\cdot\vec{\delta}/2) = 0$ is very simple. We find that the excitation energy is

$$\mathcal{E}_{ZB} = \Gamma^{(1)}[2z(1 + \beta) - (1 + 3\beta)] \tag{25a}$$

for states with neighboring spin-deviations, i.e., $\varphi_{ZB}(\vec{R}) = \delta(\vec{R}, \vec{\delta})$. For the states with spin-deviations on the same ion or non-neighboring ions, $\varphi_{ZB}(\vec{R}) = 1 - \delta(\vec{R}, \vec{\delta})$, the excitation energy is

$$\mathcal{E}_{ZB} = 2z\Gamma^{(1)}(1 + \beta) . \tag{25b}$$

Note that the neighboring-ion excitation is energetically favored only if $1 + 3\beta > 0$, and then the binding energy is equal to $\Gamma^{(1)}(1 + 3\beta)$. When $1 + 3\beta < 0$, the energy for neighboring-ion excitation is higher by $\Gamma^{(1)}|1 + 3\beta|$ than the single-ion and non-neighboring-ion excitations.

To solve Eq. (22) for the total wave vector $\vec{K}$ within the Brillouin zone, we use the standard Green's-function method. That is, we introduce a Green's function

$$D_{\vec{K}}(\vec{R}) \equiv \frac{1}{N}\sum_{\vec{p}} \frac{\cos(\vec{p}\cdot\vec{R})}{2(\Gamma^{(1)} + \Gamma^{(2)})[z - \sum_{\vec{\delta}} \cos(\vec{K}\cdot\vec{\delta}/2)\cos(\vec{p}\cdot\vec{\delta})] - \mathcal{E}} , \tag{26a}$$

and show that it satisfies the equation

$$\mathcal{H}_0 D_{\vec{K}}(\vec{R}) - \mathcal{E} D_{\vec{K}}(\vec{R}) = \delta(\vec{R}, 0) . \tag{26b}$$

Hence the solution for Eq. (22) $\varphi_{\vec{K}}(\vec{R})$ must be a linear combination of the $D_{\vec{K}}(\vec{R})$. We assume that the form for $\varphi_{\vec{K}}(\vec{R})$ is

$$\varphi_{\vec{K}}(\vec{R}) = \sum_{\vec{R}'} A_{\vec{K}}(\vec{R}') D_{\vec{K}}(\vec{R} - \vec{R}') . \tag{27}$$

By substituting Eq. (27) into Eq. (22), and by using Eq. (26b), we find

$$A_{\vec{K}}(\vec{\delta}) = -\tilde{V}\varphi_{\vec{K}}(\vec{\delta}) = \Gamma^{(1)} f(\vec{\delta}) , \tag{28a}$$

$$A_{\vec{K}}(0) = -\tilde{V}\varphi_{\vec{K}}(0) = -\Gamma^{(1)} \sum_{\vec{\delta}} \cos\left(\frac{\vec{K}\cdot\vec{\delta}}{2}\right) f(\vec{\delta}) , \tag{28b}$$

and

$$A_{\vec{K}}(\vec{R}) = 0 \quad \text{if } \vec{R} \neq 0, \ \vec{R} \neq \vec{\delta} . \tag{28c}$$

When we place the coefficients in Eqs. (28) into Eq. (27) and consider only lattices with inversion symmetry, we reduce the set of N equations, Eq. (22), into a set of $\frac{1}{2}z + 1$ equations for $\frac{1}{2}z + 1$ non-

vanishing coefficients $A_0 = A_{\vec{K}}(0)$ and $A_j = A_{\vec{K}}(\vec{\delta}_j)$ $(j = 1, \ldots, \frac{1}{2}z)$. The equations can be written in the form:

$$(\underline{1} + \underline{M})\underline{A} = 0 , \tag{29}$$

where $\underline{1}$ is a $(\frac{1}{2}z+1)\times(\frac{1}{2}z+1)$ unit matrix, $\underline{A}$ is a $(\frac{1}{2}z+1)\times 1$ column matrix, with elements A_i $(i = 0, 1, \ldots, \frac{1}{2}z)$. $\underline{M}$ is a $(\frac{1}{2}z+1)\times(\frac{1}{2}z+1)$ matrix whose elements are

$$M_{00} = 0 , \tag{30a}$$

$$M_{0i} = 2\alpha_i \quad (i = 1, \ldots, \tfrac{1}{2}z) , \tag{30b}$$

$$M_{i0} = -[(1+3\beta)D_i - 4\beta\alpha_i D_0]/2z(1+\beta) \quad (i = 1, \ldots, \tfrac{1}{2}z) , \tag{30c}$$

$$M_{ij} = -[(1+3\beta)D_{ij} - 4\beta\alpha_i D_j]/z(1+\beta) \quad (i, j = 1, \ldots, \tfrac{1}{2}z) , \tag{30d}$$

where

$$\alpha_i \equiv \cos\left(\frac{\vec{K}\cdot\vec{\delta}_i}{2}\right) \quad (i = 1, \ldots, \tfrac{1}{2}z) , \tag{31}$$

$$D_{\nu\mu} = \frac{1}{N}\sum_{\vec{\rho}} \frac{\cos[(1-\delta_{\nu 0})\vec{\rho}\cdot\vec{\delta}_\nu]\cos[(1-\delta_{\mu 0})\vec{\rho}\cdot\vec{\delta}_\mu]}{t - (2/z)\sum_{l=1,\ldots,z/2}\alpha_l\cos(\vec{\rho}\cdot\vec{\delta}_l)} , \tag{32a}$$

$$D_\nu = D_{0\nu} = D_{\nu 0} , \tag{32b}$$

and

$$t = 1 - \mathcal{E}/2z\Gamma^{(1)}(1+\beta) . \tag{33}$$

For nontrivial solutions of A_i $(i = 0, 1, \ldots, \frac{1}{2}z)$, we require that

$$|\underline{1} + \underline{M}| = 0 . \tag{34}$$

Therefore we must solve Eq. (34) for t. Then corresponding to each solution t, we obtain the coefficients A_i by solving Eq. (29). Finally, by substituting the values of t and the A_i's into Eqs. (27) and (33), we obtain the wave function and energy of the two-span–deviation states.

III. ENERGY SPECTRA AND WAVE FUNCTIONS

In this section, we apply the formalism presented in Sec. II to obtain the energy spectra and wave functions of the two-spin–deviation states. The qualitative features of such states are the same for the different lattice structures and it is instructive to obtain analytic results whenever possible in order to obtain a clearer picture of these states. Therefore, we first obtain analytic results for a linear chain. Then we study the simple cubic lattice; for this case we use numerical methods to obtain our results.

A. Linear chain

In this subsection, we solve Eq. (29) for t and A_1/A_0 for a linear chain. The corresponding wave function Eq. (27) is obtained by substituting the value of t and A_1/A_0 into the terms entering Eq. (27) and performing a contour integration. From Eqs. (26a) and (27), we see that the wave function is given as

$$\varphi_K(R) = \frac{1}{N}\sum_\rho \frac{\cos(\rho R)[A_0 + 2A_1\cos(\rho a)]}{4\Gamma^{(1)}(1+\beta)[t - \alpha\cos(\rho a)]} , \tag{35}$$

where a is the lattice constant, and $\alpha = \cos(\frac{1}{2}Ka)$. For $z = 2$, Eq. (29) is of the form

$$A_0 + 2\alpha A_1 = 0 \tag{36a}$$

and

$$M_{10}A_0 + (1 + M_{11})A_1 = 0 , \tag{36b}$$

where we have used the fact that $M_{00} = 0$ and $M_{01} = 2\alpha$, see Eq. (30). From Eqs. (30)–(33), we find that

$$M_{10} = [4\beta\alpha D_0 - (1+3\beta)D_1]/4(1+\beta) , \tag{37a}$$

$$M_{11} = [4\beta\alpha D_1 - (1+3\beta)D_{11}]/2(1+\beta) . \tag{37b}$$

$$D_{11} = \frac{1}{N}\sum_\rho \frac{\cos^2(\rho a)}{t - \alpha\cos(\rho a)} , \tag{38a}$$

$$D_n = \frac{1}{N}\sum_\rho \frac{\cos(n\rho a)}{t - \alpha\cos(\rho a)} , \tag{38b}$$

and

$$t = 1 - \mathcal{E}/4\Gamma^{(1)}(1+\beta) . \tag{39}$$

By some algebraic manipulations of Eqs. (38), we see that the functions D_{11}, D_1 and D_0 are related in the following way:

$$\alpha D_{11} = tD_1 , \tag{40a}$$

$$\alpha D_1 = tD_0 - 1 , \tag{40b}$$

and

$$\alpha(D_{n+1} + D_{n-1}) = 2(tD_n - \delta_{n,0}) . \tag{40c}$$

For $z = 2$, and the condition for nontrivial solutions, Eq. (34) is of the form

$$1 + M_{11} - 2\alpha M_{10} = 0 . \tag{41}$$

By using Eqs. (37)–(40), this condition is written as

$$a + bD_0 = 0 , \tag{42}$$

where

$$a = (1 - 5\beta) + (1+3\beta)t/\alpha^2 \tag{42a}$$

and

$$b = [4\beta\alpha^2 - (1+3\beta)t](t - \alpha^2)/\alpha^2 . \tag{42b}$$

The analytic form of D_0 can be obtained by a contour integration. It is

$$D_0 = (t^2 - \alpha^2)^{-1/2} . \tag{43}$$

For energies outside the band, $|t| > \alpha$,

$$D_0 = \pm 1/(t^2 - \alpha^2)^{1/2} , \tag{43a}$$

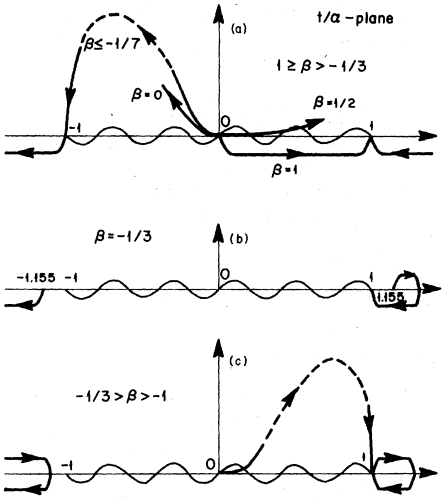

FIG. 1. Location of solutions to the bound-state condition, Eq. (42), in the upper half t/α-plane; for (a) $1>\beta>-\frac{1}{3}$, (b) $\beta=-\frac{1}{3}$, (c) $-\frac{1}{3}>\beta>-1$. The lines parallel to the real axis represent the real solutions on the physical sheet. The solid lines and the connecting broken lines in the upper half of the plane represent the complex solutions on the unphysical sheet. The broken lines represent the schematic interpolation between the complex solutions represented by the solid lines. The arrows indicate the direction of increasing α. The branch cuts are represented by the wavy line. In (b), the real solution below the band increases from 1.155 to a maximum value and then decreases to 1 as α increases from 0 to 1. In (c), the real solution below the band increases from 1 to a maximum value and then drops back to 1 as α increases from α_2 to 1.

where the plus sign is used below the band ($t>\alpha$), and the minus is used above the band ($t<-\alpha$). Inside the band, $|t|<\alpha$,

$$D_0=\pm i/(\alpha^2-t^2)^{1/2}, \tag{43b}$$

where the plus and minus signs are used above and below the branch cut, respectively. From Eqs. (27), (36a), and (40c), we see that the wave function in Eq. (35) is of the form:

$$\varphi_K(na)=\frac{A_1}{2\Gamma^{(1)}(1+\beta)\alpha}\left[(t-\alpha^2)D_n-\delta_{n,0}\right]. \tag{35a}$$

By performing a contour integration, one can easily obtain

$$D_n=\left[\frac{t}{\alpha}-\left(\frac{t^2}{\alpha^2}-1\right)^{1/2}\right]^{|n|}\Big/(t^2-\alpha^2)^{1/2}, \tag{44}$$

so that the wave function as a function of t is given as

$$\varphi_K(na)=\frac{A_1}{2\Gamma^{(1)}(1+\beta)\alpha}\left\{\frac{(t-\alpha^2)}{(t^2-\alpha^2)^{1/2}}\times\left[\frac{t}{\alpha}-\left(\frac{t^2}{\alpha^2}-1\right)^{1/2}\right]^{|n|}-\delta_{n,0}\right\}. \tag{45}$$

By using the various forms for D_0, Eqs. (43), we solve Eq. (42) for t. We find that for each given value of α and β, either there are two real solutions for t on the physical sheet, one above and one below the band, or there is one real solution on the physical sheet and one pair of complex conjugate solutions on the unphysical sheet, see Fig. 1. We will consider the following regimes of β values separately. (i) $1>\beta>-\frac{1}{3}$; (ii) $\beta=-\frac{1}{3}$; (iii) $-\frac{1}{3}>\beta>-1$.

(i) $1>\beta>-\frac{1}{3}$. For each value of α there is one real solution for t below the band on the physical sheet. This corresponds to the exchange bound states,[14,15] whose wave function has its maximum amplitude at nearest-neighbor separation, i.e., $R=a$:

$$\varphi_K(na)=\frac{A_1}{2\Gamma^{(1)}(1+\beta)\alpha}\left[\frac{(t-\alpha^2)}{(t^2-\alpha^2)^{1/2}}e^{-|n|q}-\delta_{n,0}\right], \tag{46}$$

where

$$q=\ln\left(\frac{t}{\alpha}+(t^2/\alpha^2-1)^{1/2}\right). \tag{46a}$$

The excitation energy of these states is obtained by using Eq. (39) and is shown in Fig. 2 by the thin solid lines for $\beta=0$, 0.5, and 1, respectively. We note that the exchange bound states move away from the band as β increases. For $\beta=1$, these states have a simple dispersion relation and wave function,

$$\mathcal{E}=2\Gamma^{(1)}(1-\cos Ka), \tag{47a}$$

$$\varphi_K(na)\propto e^{-|n|q}-\delta_{n,0}, \tag{47b}$$

where

$$q=\ln(1/\alpha). \tag{47c}$$

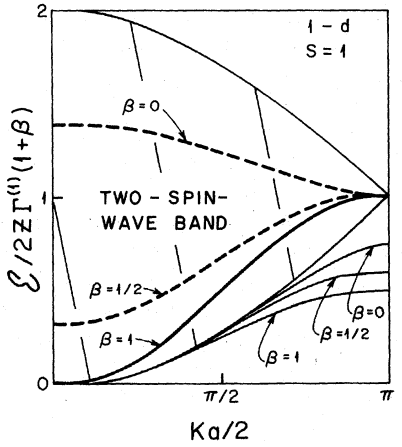

FIG. 2. Two-spin–deviation spectra for a linear chain for $\beta=0$, $\frac{1}{2}$, and 1. The broken lines in the band represent the quadrupolar resonant states. The thick solid line in the band represents the quadrupole wave dispersion curve. The thin solid lines below the band represent the exchange bound states.

Within the band on the unphysical sheet, there is a pair of complex conjugate solutions for t for $0 < \alpha \leq \alpha_1$ where $\alpha_1 = -(1+3\beta)/4\beta$ if $\beta < -\frac{1}{7}$ and $\alpha_1 = 1$ if $\beta > -\frac{1}{7}$ [see Fig. 1(a)]. The solutions with small imaginary parts correspond to quadrupolar (single-ion) resonant states; their wave functions have a damped oscillatory character.

$$\varphi_K(na) = \frac{A_1}{2\Gamma^{(1)}(1+\beta)\alpha}\left[\frac{(t-\alpha^2)}{(\alpha^2-t^2)^{1/2}}e^{-|n|q+i|n|\theta} - \delta_{n,0}\right], \tag{48a}$$

where

$$\theta = \cos^{-1}(|t_r|/\alpha), \tag{48b}$$

and

$$q = \ln[1 + |t_i|/(\alpha^2 - t_r^2)^{1/2}], \tag{48c}$$

where t_r and t_i are, respectively, the real and imaginary parts of the solution t. We note in Fig. 1(a) that, for a given value of α, t_r increases and t_i decreases monotonically with increasing β, i.e., the resonant states move to lower positions in the band and have longer lifetimes as β increases. In Fig. 2, we show the dispersion curve of the resonant states by broken lines within the band for $\beta = 0$ and 0.5. As β approaches one, the resonant states become pure quadrupolar excitation states and their dispersion relation is given as

$$\mathcal{E} = 4\Gamma^{(1)}(1 - \cos Ka). \tag{49}$$

This spectrum is shown in Fig. 2 by the thick solid line in the band. We note this energy is twice the energy of the exchange bound state Eq. (47a). For such a state, two spin deviations on a single-ion propagate together through the lattice with wave vector $\vec{K}$. As mentioned in Sec. I, we call this a quadrupole wave. The dispersion relation of the quadrupole wave is the same as that of the spin wave and it is gapless at the zone center. As discussed in Appendix A, this is a new Goldstone mode of the system due to the SU(3) symmetry of the Hamiltonian when $\beta = 1$.

From Fig. 1(a) we also note that, for a given value of β, $|t_r|/\alpha$ decreases monotonically with decreasing α for the range of β, $1 > \beta > -\frac{1}{3}$. When $1 > \beta > -\frac{1}{7}$, $|t_i|/\alpha$ decreases monotonically to zero as α decreases to zero. That is, the resonant state energy moves towards the center of the band and its lifetime becomes longer as the zone boundary is approached. When $-\frac{1}{7} \geq \beta > -\frac{1}{3}$, $|t_i|/\alpha = 0$ for $1 \geq \alpha \geq \alpha_1$. As α decreases from α_1 to zero, $|t_i|/\alpha$ rises sharply and then drops slowly back to zero. Therefore, there are no resonant states near the threshold α_1, although they exist near the zone boundary.[16] The real solutions of t for $1 \geq \alpha > \alpha_1$ correspond to bound states above the band. Their presence is due to the repulsive interaction between spin waves, Eq. (24), and their wave functions are given as

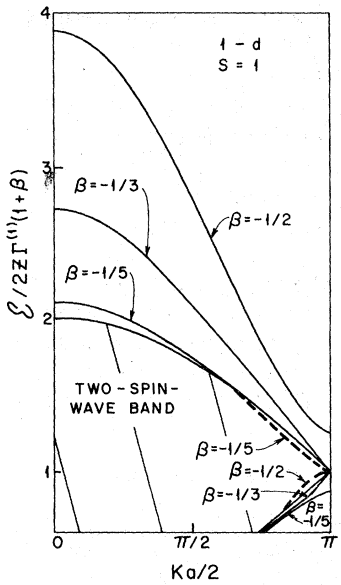

FIG. 3. Two-spin–deviation spectra for a linear chain for $\beta = -\frac{1}{5}$, $-\frac{1}{3}$, and $-\frac{1}{2}$. The broken lines within the band close to the zone boundary represent the quadrupolar resonant states. The thin solid lines represent the bound states outside the band.

$$\varphi_K(na) = \frac{-A_1}{2\Gamma^{(1)}(1+\beta)\alpha} \times \left[(-1)^{|n|}e^{-|n|q}\frac{(|t|+\alpha^2)}{(t^2-\alpha^2)^{1/2}} + \delta_{n,0}\right], \tag{50}$$

where

$$q = \ln\left(\frac{|t|}{\alpha} + (t^2/\alpha^2 - 1)\right)^{1/2}. \tag{50a}$$

The two-spin–derivative spectrum for $\beta = -0.2$ is shown in Fig. 3.

(ii) $\beta = -\frac{1}{3}$. There are two real solutions on the physical sheet, one above and one below the band, see Fig. 1(b):

$$t = \tfrac{1}{3}\alpha\left[-\alpha \pm 2\sqrt{3+\alpha^2}\right]. \tag{51}$$

The plus and minus signs are for the bound states below and above the band, respectively. The wave functions for these bound states are given by Eqs. (46) and (50). At the zone boundary all the energy levels are degenerate. The spectrum for $\beta = -\frac{1}{3}$ is shown in Fig. 3.

(iii) $-\frac{1}{3} > \beta > -1$. Below the band, there is one real solution for t on the physical sheet for $1 > \alpha > \alpha_2 = (1+3\beta)/4\beta$. The wave function of this bound state is given by Eq. (46). The degree of localization depends on the relative binding energy. At $\alpha = 1$ and $\alpha = \alpha_2$, the wave function is spread out. When $0 < \alpha < \alpha_2$, there is a pair of complex conjugate solutions for t connected to the real solution at $\alpha = \alpha_2$, see Fig. 1(c). The imaginary part of t/α is small only when $\alpha \sim 0$. Hence, resonant states exist only near the zone boundary. These states are represented by the broken line in the band in Fig. 3.

Above the band, there is one real solution for t on the physical sheet for each value of α. This also corresponds to bound states which have localized wave functions as a result of the repulsive nature of the spin-wave interaction, Eq. (24). However, these states are different from the exchange bound states below the band found by Wortis[14] and Hanus[15] in the following way. Although the two spin deviations are sharply localized on neighboring ions at the zone boundary, they are more localized on a single ion as the zone center is approached. The excitation energies of these states are represented by the solid line above the band in Fig. 3. As β decreases, such a state moves further away from the band.

B. Simple-cubic lattice

In this subsection, we consider the case of a simple-cubic lattice for which $z=6$. For the total wave vector $\vec{K}$ of the two-spin–derivation states along the cubic diagonal, i.e., $\vec{K}=K(1,1,1)$, Eq. (29) is of the form,

$$\begin{bmatrix} 1 & 2\alpha & 2\alpha & 2\alpha \\ M_{10} & 1+M_{11} & M_{12} & M_{12} \\ M_{10} & M_{12} & 1+M_{11} & M_{12} \\ M_{10} & M_{12} & M_{12} & 1+M_{11} \end{bmatrix} \begin{bmatrix} A_0 \\ A_1 \\ A_2 \\ A_3 \end{bmatrix} = 0 , \quad (52)$$

where from Eq. (30b)

$$\alpha = \cos\tfrac{1}{2}Ka , \quad (53a)$$

and from Eqs. (30)–(33)

$$M_{10} = [4\beta\alpha D_0 - (1+3\beta)D_1]/12(1+\beta) , \quad (53b)$$

$$M_{1\mu} = [4\beta\alpha D_1 - (1+3\beta)D_{1\mu}]/6(1+\beta) \ (\mu = 1, 2), \quad (53c)$$

$$D_{1\mu} = \frac{1}{N}\sum_{\rho_1\rho_2\rho_3} \frac{\cos\rho_1 \cos\rho_\mu}{t - \alpha(\cos\rho_1 + \cos\rho_2 + \cos\rho_3)/3} , \quad (53d)$$

and

$$D_n = \frac{1}{N}\sum_{\rho_1\rho_2\rho_3} \frac{\cos(n\rho_1)}{t - \alpha(\cos\rho_1 + \cos\rho_2 + \cos\rho_3)/3} . \quad (53e)$$

The functions D are related in the following way:

$$\alpha(D_{11} + 2D_{12}) = 3tD_1 \quad (54a)$$

and

$$\alpha D_1 = tD_0 - 1. \quad (54b)$$

The matrix Eq. (52) has nontrivial solutions if the following condition is satisfied

$$(1 + M_{11} - M_{12})^2 (1 + M_{11} + 2M_{12} - 6\alpha M_{10}) = 0 . \quad (55)$$

This agrees with the bound state conditions obtained by Pink and Tremblay[2] from the location of the poles of the double-time Green's function. In Appendix C, we show that the wave function of the bound states satisfying the condition

$$1 + M_{11} + 2M_{12} - 6\alpha M_{10} = 0 \quad (56a)$$

have s-symmetry wave functions, while the wave function satisfying the condition

$$1 + M_{11} - M_{12} = 0 \quad (56b)$$

has d-wave character. The d-wave amplitude is zero for zero separation of the two spin deviations, $\vec{R}=0$, while by definition the wave functions for single-ion excitions have a finite amplitude at zero separation. As we show in Appendix C, the quadrupolar interaction $\mathcal{H}^{(2)}$ does not mix the d-wave solutions with either the s-wave or the single-ion solutions. However, it does mix the s-wave and single-ion solutions. Silberglitt and Torrance,[12] who studied the effects of single-ion anisotropy on two-spin-wave spectra, were the first to observe that the d-wave bound states did not mix with either the s-wave or single-ion bound states. By using Eqs. (53), the s-wave condition, Eq. (56b) is reduced to the form

$$a + bD_0 = 0 , \quad (57)$$

where a and b are given by Eqs. (42a) and (42b). This equation looks the same as Eq. (42) except that here D_0 is a three-dimensional integral, Eq. (53e). We have calculated the values of D_0 for $|t/\alpha| > 1$ by using the numerical method of Chebyshev interpolation[17] and we have solved Eq. (57) for t. From the relation between t and excitation energy $\mathcal{E}$, Eq. (33), we have obtained the energy spectrum of the s-wave bound states for given values of β and α.

The d-wave condition, Eq. (56a) can be reduced to the form:

$$6(1+\beta) - (1+3\beta)(D_{11} - D_{12}) = 0 . \quad (58)$$

By using the tables of lattice Green's functions by Maradudin *et al.*[18] for the functions D_{11} and D_{12}, we solved Eq. (51) for t outside the band for given values of β and α. From the relation Eq. (33), we have obtained the energy spectra of the d-wave bound states.

As in the one-dimensional case, there exist quadrupolar (single-ion) resonant states in the two-spin-wave band for the simple-cubic lattice. We obtain the energies of these resonant states from the location of the peaks in the spectral density of states of quadrupolar excitations which are calculated in Sec. IV. Here we present the results for the energy spectra of the bound states outside the band and the resonant states within the band for two regimes of β: (i) $1 \geq \beta \geq -\frac{1}{3}$; (ii) $-\frac{1}{3} > \beta > -1$.

(i) $1 \geq \beta \geq -\frac{1}{3}$. For a given value of β, we find that below the band there are s-wave exchange bound states for $\alpha_s > \alpha \geq 0$, and doubly degenerate d-wave exchange bound states for $\alpha_d > \alpha \geq 0$, where

$$\alpha_s = \{[(1+7\beta)C + (1-5\beta)] + \{[(1+7\beta)C + (1-5\beta)]^2$$

$$-16\beta C(C-1)(1+3\beta)\}^{1/2})/8\beta C\,, \qquad (59)$$

where $C \cong 1.5164$, and

$$\alpha_d = 0.093(1+3\beta)/(1+\beta). \qquad (60)$$

Note that $\alpha_s > \alpha_d$. For $\beta > -\frac{1}{3}$ both α_s and α_d are increasing functions of β. For example, at $\beta = -\frac{1}{3}$, $\alpha_s = \alpha_d = 0$; while for $\beta = 1$, $\alpha_s = 0.33$, and $\alpha_d = 0.186$. This implies that as β increases, the exchange bound state exists below the band over an increasingly larger fraction of the Brillouin zone. We also find that the relative binding energy of these bound states becomes stronger as β increases. In Fig. 4, we show the energy spectra of these exchange bound states by the thin solid lines for the case of $\beta = \frac{1}{2}$.

In addition to the bound states below the band we have found that in the small interval $-\frac{1}{3} < \beta < \beta_1$, where $\beta_1 = C/(4-7C) \simeq -0.23$, s-wave bound states appear *above* the band for $1 \geq \alpha > \alpha_1 > 0$, where

$$\alpha_1 = -([(1+7\beta)C + (1-5\beta)] + \{[(1+7\beta)C + (1-5\beta)]^2 - 16\beta C(C-1)(1+3\beta)\}^{1/2})/8\beta C\,. \qquad (61)$$

We note that α_1 also decreases monotonically with decreasing β; for $\beta = -\frac{1}{3}$, $\alpha_1 = (2-C)/C \simeq 0.33$. Therefore, s-wave bound states exist above the band for the total wave vector K less than the threshold value $K_1 = (2/a)\cos^{-1}\alpha_1$. Their wave functions are localized. The degree of spatial localization decreases with α. At the threshold value α_1, the wave function is spread out.

Within the band, there are quadrupolar resonant states with wave functions which have a damped oscillatory character. Such states are represented by the broken line in Fig. 4 for $\beta = 0.5$. Note that these states connect to the tip of the band at the zone boundary. In the rest of the Brillouin zone, however, they move to lower positions in the band as β increases. As β approaches one, they become

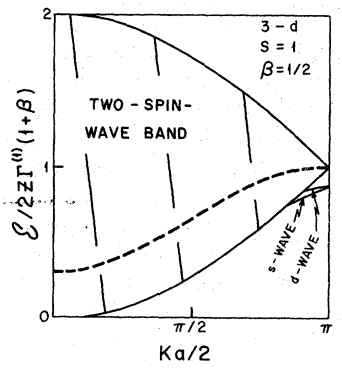

FIG. 4. Two-spin–deviation spectra for a simple-cubic lattice for $\beta = \frac{1}{2}$. The broken line in the band represents the quadrupolar resonant states. The solid lines below the band represent the s-wave and d-wave exchange bound states.

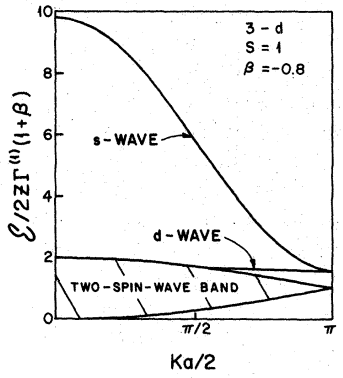

FIG. 5. Two-spin–deviation spectra for a simple-cubic lattice for $\beta = -0.8$. The thin solid lines represent the exchange bound states above the band.

eigenstates and their dispersion relation is given as

$$\mathcal{E} = 12\Gamma^{(1)}(1 - \cos Ka)\,.$$

This energy is just three times the energy for the case of the linear chain, Eq. (49), due to the fact that $z = 6$ in the simple-cubic lattice, and $z = 2$ in the linear chain. The character of these states is exactly the same as in the one-dimensional case. That is, it is degenerate with the spin-wave mode and is gapless at the zone center. It is a new Goldstone mode of the system due to the SU(3) symmetry of the Hamiltonian for $\beta = 1$, see Appendix A.

(ii) $-\frac{1}{3} > \beta > -1$. In this regime, there are no bound states below the band nor resonant states within the band. Above the band, there are doubly degenerate d-wave exchange bound states for $\alpha_d' > \alpha \geq 0$, where $\alpha_d' = -\alpha_d$ if $|\alpha_d| < 1$, and $\alpha_d' = 1$ if $|\alpha_d| > 1$, where α_d is given by Eq. (60). From Eq. (60), we note that α_d' increases monotonically with decreasing β, until $\beta \cong -0.86$ for which $|\alpha_d| = 1$. This implies that the d-wave bound states only exist above the band for the total wave vector $\vec{K}$ larger than some threshold value when $\beta > -0.86$, while for $\beta < -0.86$ they exist over the entire Brillouin zone.

There are also s-wave bound states above the band over the entire Brillouin zone when $\beta < -0.36$. For $-\frac{1}{3} > \beta > -0.36$, we find that s-wave bound states do not exist over a small intermediate region of the Brillouin zone. In Fig. 5 we show the spectrum for $\beta = -0.8$. We see that the dispersion curve of the d-wave bound states is rather flat.

IV. DENSITY OF STATES

The effect of quadrupolar interactions on the elementary excitations can be seen in the spectral density of states of the quadrupolar excitations. These are two-spin–deviation excitations, $m = 2$,

that occur at the same site. In this section we will show that the single-ion (quadrupolar) resonant state is seen as a sharp peak in the density of states. As one increases β, the linewidth of the peak decreases and the peak moves to a lower position in the band. At the zone center, the spectral density of states of quadrupolar excitations may be observed by Raman scattering. Mechanisms for these quadrupolar excitations have been derived by Moriya, [8] Elliott and Loudon, [9] and Thorpe. [10]

To calculate the spectral density of states of the quadrupolar excitations we introduce the Green's function

$$G_2(i, i'; j, j'; t) \equiv -i\theta(t)\langle A^\dagger(i, i'; 0) A(j, j'; t)\rangle_g \tag{62}$$

where

$$A(i, i'; t) = s_i^-(t)\, s_{i'}^-(t)\,, \tag{62a}$$

and $\theta(t)$ is the unit step function. The expectation value of the operators is taken over the ground-state configuration of the system. (This Green's function is of a more general form than will be needed to study the spectral density of states of quadrupolar excitations. It has the advantage that one can use the expressions we develop to obtain the Green's function for two-spin-deviation excitations at *different* sites.) When $i = i'$ and $j = j'$ we note from Eq. (3b) that A is related to the quadrupolar operator, $\mathcal{O}_2^2$, as follows.

$$A(i, i) = 2\mathcal{O}_{-2}^2(i)\,, \tag{63}$$

and the Green's function for quadrupolar excitations is

$$G_2(i, i; j, j; t) = -4i\,\theta(t)\langle \mathcal{O}_2^2(i, 0)\, \mathcal{O}_{-2}^2(j, t)\rangle_g\,. \tag{63a}$$

As our system is translationally invariant, we define a Green's function that has been partially Fourier transformed

$$G_2(\vec{\rho}_i, \vec{\rho}_j; \vec{K}, \mathcal{E}) \equiv \sum_{\vec{r}_j + \vec{r}_{j'}, \vec{r}_i + \vec{r}_{i'}} e^{i\vec{K}\cdot(\vec{r}_j + \vec{r}_{j'} - \vec{r}_i - \vec{r}_{i'})/2} \int dt\, e^{-i\mathcal{E}t}\, G_2(i, i'; j, j'; t)\,, \tag{64}$$

where $\vec{\rho}_j = \vec{r}_{j'} - \vec{r}_j$ and $\vec{\rho}_i = \vec{r}_{i'} - \vec{r}_i$ represent the separation between the two sites at which the spin deviations occur. By using the spin commutation relations and the identity Eq. (19), we find that these Green's functions obey the following equation

$$\begin{aligned}[2z\Gamma^{(1)}(1+\beta) - \mathcal{E}]\, G_2(\vec{\rho}_i, \vec{\rho}_j) - \Gamma^{(1)}(1+\beta)\sum_{\vec{\delta}'} \cos(\tfrac{1}{2}\vec{K}\cdot\vec{\delta}')\,[G_2(\vec{\rho}_i, \vec{\rho}_j + \vec{\delta}') + G_2(\vec{\rho}_i, \vec{\rho}_j - \vec{\delta}')] \\ - \Gamma^{(1)}\Big(F(\vec{\delta})\,\delta(\vec{\rho}_j, \vec{\delta}) - \vec{\delta}(\vec{\rho}_j, 0)\sum_{\vec{\delta}'} \cos(\tfrac{1}{2}\vec{K}\cdot\vec{\delta}')\, F(\vec{\delta}')\Big) = 4[\tfrac{1}{2}\delta(\vec{\rho}_i, 0) - 1][\delta(\vec{\rho}_i, \vec{\rho}_j) + \delta(\vec{\rho}_i, -\vec{\rho}_j)]\,,\end{aligned} \tag{65}$$

where

$$F(\vec{\rho}) = (1+3\beta)\, G_2(\vec{\rho}_i, \vec{\rho}) - 4\beta\cos(\tfrac{1}{2}\vec{K}\cdot\vec{\rho})\, G_2(\vec{\rho}_i, 0)\,. \tag{65a}$$

The last term on the left-hand side of Eq. (65) is the manifestation of the interaction between a pair of spin waves with total wave vector $\vec{K}$. Note in the special case of $\beta = 0$ Eq. (65) agrees with Eq. (3.6) in Ref. 10. By following the method used by Thorpe, [10] we solve Eq. (65) and obtain the expression for the quadrupolar Green's function $G_2(0, 0)$. For a $\frac{1}{2}z$-dimensional hypercubic lattice and for the total wave vector $\vec{K}$ along the hypercube diagonal, we find that

$$G_2(0, 0) = \frac{2[(1+3\beta)\, D_1 - 2(1+\beta)\,\alpha D_0]}{z\Gamma^{(1)}(1+\beta)\alpha(a + b\, D_0)}\,, \tag{66}$$

where $\alpha = \cos(\frac{1}{2}Ka)$ and K is the magnitude of each component of $\vec{K}$.

The spectral density of states for the quadrupolar excitations is related to the imaginary part of the quadrupolar Green's function $G_2(0, 0)$, (66).

$$\mathfrak{D}(\vec{K}, \mathcal{E}) \equiv \frac{z\Gamma^{(1)}(1+\beta)}{2\pi}\, \mathrm{Im} G_2(0, 0; \vec{K}, \mathcal{E})\,. \tag{67}$$

A. Linear chain

For a linear chain we obtain an analytic expression for the quadrupolar Green's function:

$$G_2(0, 0) = \frac{2\alpha^2(1-\beta)^2\,(t^2 - \alpha^2)^{1/2} - u(t)}{\Gamma^{(1)}(1+\beta)\,\Delta(t)}\,, \tag{68}$$

where

$$\Delta(t) = a_0 + a_1 t + a_2 t^2 + a_3 t^3\,, \tag{68a}$$

$$u(t) = a_3 t^2 + a_4 t + a_5\,, \tag{68b}$$

$$a_0 = \alpha^4[(1-5\beta)^2 + 16\beta^2\alpha^2]\,, \tag{69a}$$

$$a_1 = 2\alpha^2(1+3\beta)(1-5\beta) - 8\beta\alpha^4(1+7\beta)\,, \tag{69b}$$

$$a_2 = (1+3\beta)^2 + 16\beta\alpha^2(2+3\beta)\,, \tag{69c}$$

$$a_3 = -4(1+\beta)(1+3\beta)\,, \tag{69d}$$

$$a_4 = (1+3\beta)^2 + 2\alpha^2(1+10\beta+13\beta^2)\,, \tag{69e}$$

and

$$a_5 = \alpha^2(1+3\beta)(1-5\beta) - 8\beta\alpha^4(1+\beta)\,. \tag{69f}$$

In the special case of $\beta = 0$, the expression in Eq. (68) agrees with Eq. (H. 20) in Ref. 19 by Wortis. Inside the band, $|t| < \alpha$, we find the density of states

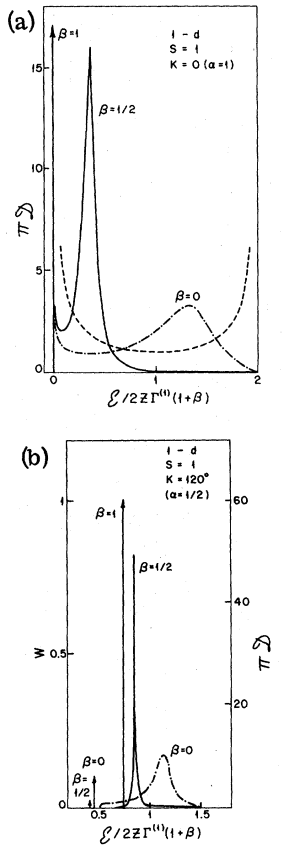

FIG. 6. Density-of-states curves for a linear chain for $\beta = 0$, $\frac{1}{2}$, and 1; and for (a) $\alpha = 1$, (b) $\alpha = \frac{1}{2}$. The broken lines represent the density of states for non-interacting spin waves. The chain and solid lines are respectively for the cases of $\beta = 0$ and 0.5. We note that the peak becomes sharper and lies at a lower position in the band as β increases. For $\beta = 1$, the density of states is just the delta function shown by the arrow. In (b), there are also arrows below the band representing the exchange bound states. The length of an arrow represents the weight associated with the bound state.

states is

$$\mathfrak{D} = 2\alpha^2(1-\beta)^2\,(t^2-\alpha^2)^{1/2}/\pi\Delta(t)\,. \tag{70}$$

The density of states outside the band, $|t| > \alpha$, is given as

$$\mathfrak{D} = \sum_i W(t_i)\,\delta(t-t_i)\,, \tag{71}$$

where t_i is the value of t for a bound state $[\Delta(t_i) = 0]$. The weight of the bound state is given by

$$W(t) = \left| \frac{u(t) \mp 2\alpha^2(1-\beta)^2(t^2-\alpha^2)^{1/2}}{\Delta'(t)} \right| \tag{72a}$$

for the case when $\Delta'(t_i) \equiv (d\Delta/dt)_{t=t_i}$ is nonzero. If $\Delta'(t_i) = 0$ but the second derivative $\Delta''(t_i)$ is nonzero we have

$$W(t) = \left| \frac{u'(t) \mp 2\alpha^2(1-\beta)^2\, t/(t^2-\alpha^2)^{1/2}}{\Delta''(t)} \right|\,, \tag{72b}$$

where $u'(t) = du/dt$. The minus and plus signs in Eqs. (72) are for below and above the band respectively.

The density of states curves for the linear chain are plotted in Figs. 6 and 7. For non-interacting spin waves the density of states is given as

$$\mathfrak{D}_{NI} = \frac{1}{\pi(\alpha^2 - t^2)^{1/2}} \tag{73}$$

and is shown in Fig. 6(a) by the broken lines. We note that the interaction between spin waves drastically changes the density of states even when no quadrupolar interactions are present, i.e., $\beta = 0$. As β increases the resonant peak becomes sharper and lies at a lower position in the band. For $\beta = 1$, we note from Eqs. (70) and (71) that the entire density of states is just one δ function.

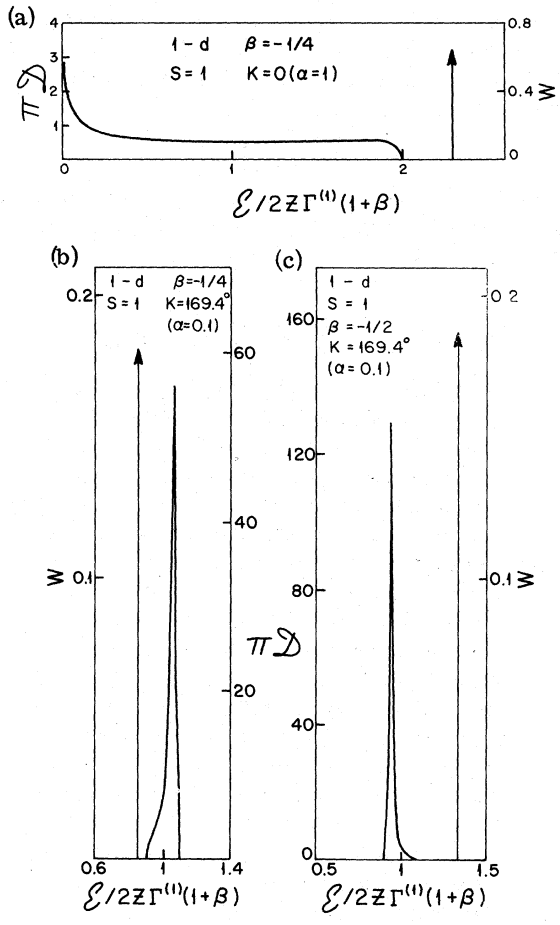

FIG. 7. Density-of-states curves for a linear chain for (a) $\beta = -\frac{1}{4}$, $\alpha = 1$, (b) $\beta = -\frac{1}{4}$, $\alpha = 0.1$, (c) $\beta = -\frac{1}{2}$, and $\alpha = 0.1$. The arrows outside the band represent the bound states whose weights are represented by the lengths of the arrows.

$$\mathfrak{D} = \delta(t - \alpha^2) \tag{74}$$

for all α. This represents the quadrupole wave mode for $\beta = 1$ and is shown by the arrow within the band in Figs. 6. The bound states for $\alpha < 1$ are shown by the arrows below the band in Fig. 6b; their length represents the weight of the bound state. In Fig. 6(a) the divergence in the density of states at zero energy is due to the fact that the bound state touches the bottom of the band at the zone center, see Fig. 2.

The density of states curves are quite different for negative β. At the zone center ($\alpha = 1$), the density of states within the band, Fig. 7(a), is greatly reduced when compared to the curves in Fig. 6a, and there is no resonant peak in this case. The bound state above the band takes on the finite weight shown by the arrow in Fig. 7(a). Near the zone boundary $\alpha = 0.1$, we find there is a very sharp resonant peak in the band and a bound state below the band for $\beta = -0.25$, see Fig. 7(b). When the quadrupolar interactions become more negative [see Fig. 7(c) for $\beta = -0.5$ and $\alpha = 0.1$], we note that the resonant peak lies below the center of the two-spin-wave band, i.e., at $t > 0$, and that the bound state lies *above* the band.

B. Simple-cubic lattice

For the simple-cubic lattice. the Green's function for quadrupolar excitations propagating along a cube diagonal, $\vec{K} = K(1, 1, 1)$, is given as

$$G_2(0, 0; \vec{K}, \mathcal{E}) = -\frac{2(1+\beta)D_0 - (1+3\beta)D_1/\alpha}{3\Gamma^{(1)}(1+\beta)(a+bD_0)}, \tag{75}$$

where $\alpha = \cos\frac{1}{2}Ka$, D_0 and D_1 are given by Eq. (53e) ($n = 0, 1$), and a and b are given by Eqs. (42a) and (42b). From Eqs. (56b) and (57) we deduce that only states with spherical symmetry (s-wave states) contribute to the spectral density of states for quadrupolar excitations. To calculate the density of states from Eq. (75) we used the table generated by Silberglitt[13] for the real part of D_0 and Baroody's formula[20] for the imaginary part of D_0 within the band. Also we used the Chebyshev interpolation method of Mannari *et al.*[17] to calculate D_0 and $\partial D_0/\partial t$ outside the band. By combining these numerical tabulations we were able to calculate the density of states for quadrupolar excitations Eq. (75), both inside and outside the band for the simple-cubic lattice.

In Figs. 8, we show the density of states curve for $\alpha = 1$ and $\alpha = 0.5$ for $\beta = 0$, 0.5 and 1. The qualitative features of the resonant peaks are the same as in Figs. 6. However, for the simple-cubic lattice the density of states for non-interacting spin waves has Van Hove singularities. These are washed out by the interaction between spin waves even in the case when $\beta = 0$.[21] In Figs. 9, we show

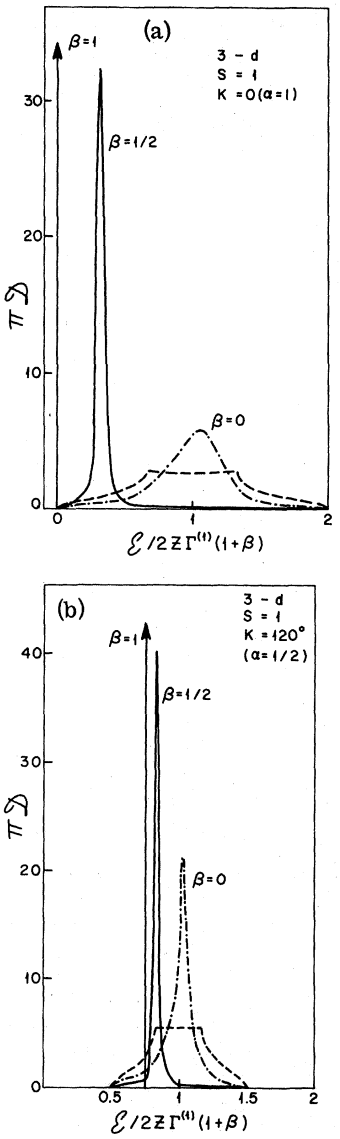

FIG. 8. Density of states curves for a simple-cubic lattice for $\beta = 0$, $\frac{1}{2}$ and 1, for (a) $\alpha = 1$, and (b) $\alpha = \frac{1}{2}$. The broken lines are for non-interacting spin waves. The chain and solid lines are for $\beta = 0$ and $\frac{1}{2}$, respectively. The arrow represents the δ-function peak of the density of states at the quadrupole wave energy for $\beta = 1$. We note that the Van Hove singularities for the non-interacting case are washed out even for $\beta = 0$. The resonant peaks are sharper for larger values of β and smaller values of α.

the density of states curve for $\alpha = 1$ and $\alpha = 0.1$ for $\beta = -0.5$. The density of states within the band in Fig. 9(a) is drastically reduced as compared with that in Fig. 8(a), and the Van Hove singularities remain. The bound state above the band takes on finite weight.

In Figs. 10 we plot the weights of the s-wave

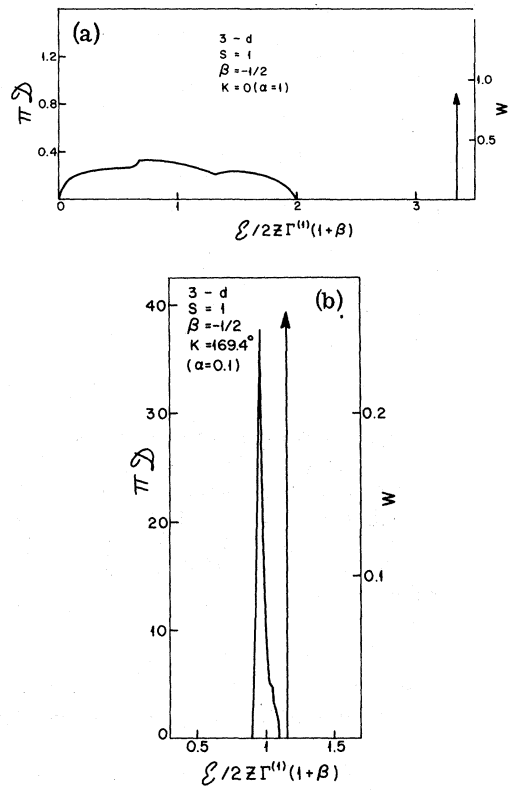

FIG. 9. Density-of-states curves for a simple-cubic lattice for $\beta = -\frac{1}{2}$ and for (a) $\alpha = 1$, (b) $\alpha = 0.1$. The arrows represent the bound states outside the band. We note that the Van Hove singularities remain in the density of states within the band.

bound states for a simple-cubic lattice for various values of α and β. We find for bound states above the band that their weight for a given value of β starts at zero and increases monotonically with α, see Fig. 10(a). For a given value of α we find that the weight $W[t_b(\alpha,\beta)]$ and the splitting of the bound states off the top of the band increases monotonically with decreasing β, see Fig. 10(b). For the bound states below the band, and for given value of β, the weight $W[t_b(\alpha, \beta)]$ increases from zero to a maximum value and then drops back to zero as α goes from zero to the threshold value α_c where the bound state merges with the bottom of the two-spin-wave band. In Fig. 10(c), we show this variation of the weight for $\beta = 0.5$. The qualitative feature of the variation of the weight with α and β in a linear chain is the same as that in a simple-cubic lattice.

V. DISCUSSION OF RESULTS

We have studied the effects of quadrupolar interactions on the elementary excitations of a spin-1 ferromagnet. The only effect of the quadrupolar interaction on the spin-wave energy is to vary the size of its dispersion. However, in the energy spectra of two-spin–deviation ($m = 2$) states, we have found that the presence of quadrupolar interactions has a marked effect. The single-ion $m = 2$ excitations, which we call quadrupolar excitations, are in general mixed together with the two-ion excitations. For the isotropic Hamiltonian the mixing occurs unless $\beta = 1$. This means that if we try to propagate a quadrupolar excitation in a solid described by the Hamiltonian Eq. (1) for $\beta < 1$, it decays into two-ion excitations. Therefore the quadrupolar excitations form resonant states within the two-spin-wave band. These quadrupolar resonant states have finite lifetimes which increase with β and the total wave vector $\vec{K}$. They are seen as distinctive peaks in the spectral density of states of quadrupolar excitations within the band. For a given value of the total wave vector $\vec{K}$, the line width of the peak decreases and the peak moves to a lower position in the band as β increases. For a given value of β, the peak moves towards the center of the band and its line width decreases to zero as the zone boundary is approached.

When $\beta = 1$ the total quadrupole moment of the solid is a good quantum number, see Appendix A. As we noted in Sec. II, the total quadrupole moment of the solid is different for quadrupolar excitations and two-ion excitations. Therefore the decay of quadrupolar excitations is forbidden for $\beta = 1$ because such a process does not conserve the total quadrupole moment of the solid. We call the eigenstate which describes the coherent propagation of the quadrupolar excitations through the solid a quadrupole wave. The spectral density of states of quadrupolar excitations has a δ-function peak at the quadrupole wave energy. We have also recognized that for this special ratio of the coupling constants, $\beta = 1$, the Hamiltonian possesses SU(3) symmetry. This manifests itself in the excitation spectrum in that the dispersion relation of quadrupole waves is identical to that of spin waves. At the zone center, $\vec{K} = 0$, the quadrupolar excitations are propagated through the solid with zero energy. This zero-energy mode is a new Goldstone boson which acts to restore the SU(3) symmetry that is broken when the ground state of the system becomes ordered.

Aside from the quadrupolar resonant states inside the two-spin-wave band, we have found that the bound states outside the band are also affected by the presence of quadrupolar interactions. Depending on the ratio of the quadrupolar coupling to dipolar coupling β, these bound states exist either above or below the band, or simultaneously both above and below the band. The bound states below the band are more strongly bound for larger values of β. When β is sufficiently negative, there is repulsive interaction between two spin waves, which causes bound states to split off above the band. This split-

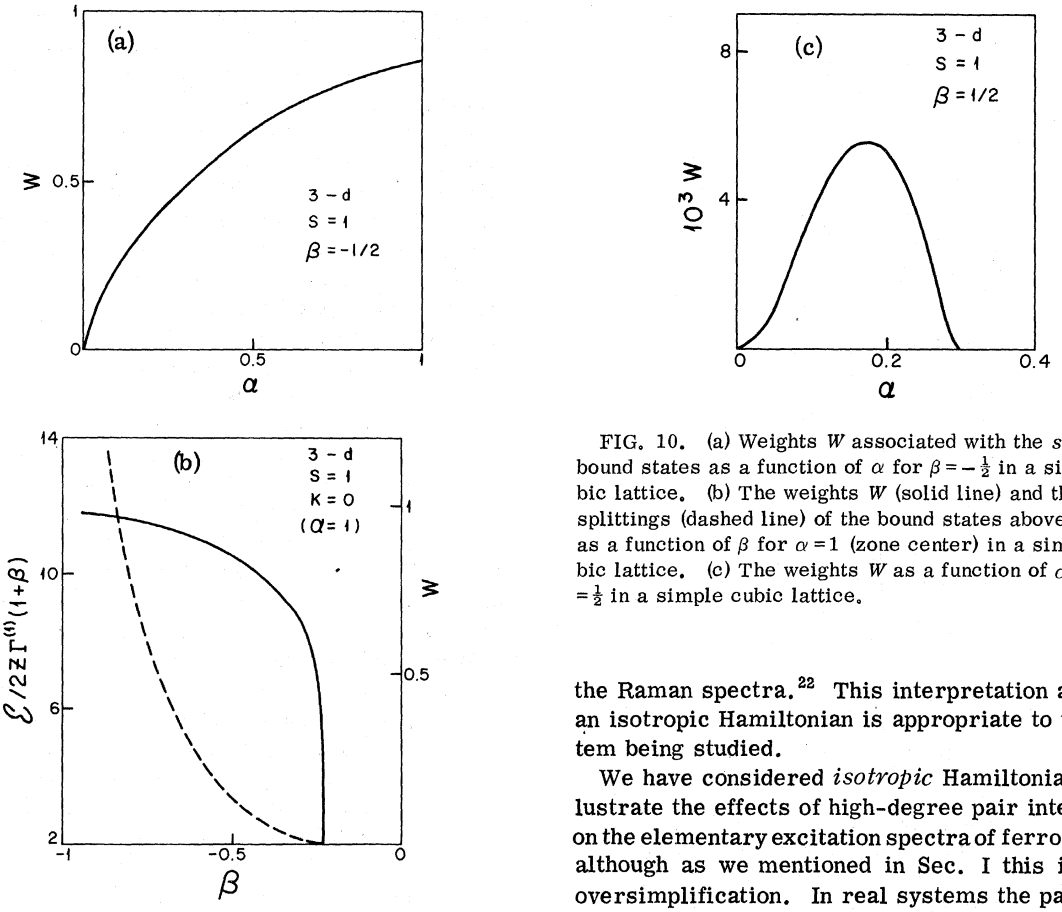

FIG. 10. (a) Weights W associated with the s-wave bound states as a function of α for $\beta = -\frac{1}{2}$ in a simple cubic lattice. (b) The weights W (solid line) and the energy splittings (dashed line) of the bound states above the band as a function of β for $\alpha = 1$ (zone center) in a simple-cubic lattice. (c) The weights W as a function of α for $\beta = \frac{1}{2}$ in a simple cubic lattice.

ting increases as β decreases, i.e., β becomes more negative. We have also calculated the weights of the spectral density of states of quadrupolar excitations associated with these bound states. We found that the d-wave bound states in a simple cubic lattice do not carry any weight in this density of states. However, the weight of the s-wave bound state above the band increases monotonically with decreasing β ($\beta < 0$) for a given value of $\vec{K}$, and it decreases monotonically with increasing $\vec{K}$ for a given value of negative β. For the s-wave bound states below the band, the weight increases from zero to a maximum value and then drops back to zero as β increases towards one, for a given value of $\vec{K}$. This weight behaves the same way if we fix the value of β and let $\vec{K}$ increase toward the zone boundary.

The zone-center density of states of quadrupolar excitations can be observed by Raman scattering. From the location and line width of the peak associated with the quadrupolar resonant state within the band, and the location and weight of the peak associated with the bound state above the band, one can in principle determine the quadrupolar coupling $\Gamma^{(2)}$ and dipolar coupling $\Gamma^{(1)}$ simultaneously from the Raman spectra.[22] This interpretation assumes an isotropic Hamiltonian is appropriate to the system being studied.

We have considered *isotropic* Hamiltonians to illustrate the effects of high-degree pair interactions on the elementary excitation spectra of ferromagnets, although as we mentioned in Sec. I this is an oversimplification. In real systems the pair interactions are generally anisotropic, e.g., for a cubic system the quadrupolar interactions must be described by at least two coupling constants. The generalization of our present calculation to ferromagnets with pair anisotropy is straightforward. Pink and Ballard[3] have studied the effects of single-ion and pair anisotropy terms on the two-spin-wave bound state spectra. In Appendix B, we study the qualitative aspects of the spectra of quadrupolar resonant states and quadrupolar waves of the Hamiltonian with pair anisotropy

$$\mathcal{H} = \sum_{\substack{l=1,2 \\ 0 \le m \le l}} \mathcal{H}_m^{(l)}, \tag{76}$$

where

$$\mathcal{H}_m^{(l)} = -\Gamma_m^{(l)} \sum_{i,j} (-1)^m [\mathcal{O}_m^l(i)\mathcal{O}_{-m}^l(j) + \mathcal{O}_{-m}^l(i)\mathcal{O}_m^l(j)]. \tag{77}$$

We find that whenever $\beta_1 \equiv \Gamma_1^{(2)}/\Gamma_1^{(1)} = 1$, a quadrupole wave is an eigenstate of the Hamiltonian, Eq. (76). The dispersion curve of the quadrupole wave may overlap with the two-spin-wave band, depending on the relative magnitudes of the five coupling constants $\Gamma_0^{(1)}$, $\Gamma_0^{(2)}$, $\Gamma_2^{(2)}$, and $\Gamma_1^{(2)} = \Gamma_1^{(1)}$, see Fig. 12(a). If $\Gamma_1^{(2)}$ deviates slightly from $\Gamma_1^{(1)}$, with the other constants fixed, there exist quadrupolar resonant states within the band.[23] The lifetime of

these resonant states decreases as $|\beta_1 - 1|$ increases, and the energy of the resonant states is shifted from the quadrupole wave energy by an amount which increases with $|\beta_1 - 1|$. These qualitative features are the same for lattices of all dimensions, although the quantitative aspects do depend on lattice structure.

In addition, in more realistic calculations of the elementary excitation spectra of Jahn-Teller system, such as the rare-earth vanadates and pnictides, one should take into account orbit-lattice coupling. Then there is a coupling of the phonons to the quadrupolar excitations. This has been discussed by Elliott *et al.*[24] for the vanadates and has recently been found in $PrAlO_3$.[25] Also, there is spin-phonon coupling which produces anticrossings in the elementary excitation spectra of Jahn-Teller systems.[26] Finally, we have restricted our discussion to the case of spin-1 ferromagnets. However, there are many systems like the rare-earth vanadates which are antiferromagnets and where the effective spin of the magnetic ion is greater than 1. Therefore it is also necessary to extend the present calculation to systems with $s > 1$ and to antiferromagnets. We are presently working on these extensions and will present our results in future publications.

ACKNOWLEDGMENTS

We want to give special thanks to Dr. Jean Sivardière for bringing this problem to our attention and for numerous fruitful conversations. We also want to thank Dr. R. Silberglitt and Dr. M. F. Thorpe for useful discussions and their helpful comments.

APPENDIX A: SYMMETRY OF HAMILTONIAN

The following is a general discussion of the symmetry properties of Hamiltonians with high-degree pair interactions; it is not restricted to spin-1 systems. We consider the Hamiltonian

$$\mathcal{H} = \sum_{l=1}^{2s} \sum_{i,j} \Gamma^{(l)}(i,j)\, \mathcal{O}^l(i) \cdot \mathcal{O}^l(j) \,. \tag{A1}$$

This Hamiltonian is written in terms of operators $\mathcal{O}^l_m$ which induce unimodular (unitary) transformations in a space of dimensions $2s+1$. These operators form a complete set of generators for an $SU(2s+1)$ continuous group algebra.[7] They also have been constructed so as to transform according to the irreducible representations (l) of O(3) or SU(2) under three-dimensional rotations. The operators $\mathcal{O}^l_m$ define a Lie algebra and therefore have well-defined commutation properties. We will use these commutation properties to classify the eigenstates of the Hamiltonian (A1). Let us define operators in momentum space as

$$\mathcal{O}^l_m(\vec{k}) \equiv \frac{1}{\sqrt{N}} \sum_i e^{-i\vec{k}\cdot\vec{R}_i} \mathcal{O}^l_m(i) \,. \tag{A2}$$

In terms of this operator the Hamiltonian (A1) is written as

$$\mathcal{H} = \sum_l \sum_{\vec{k}} \Gamma^{(l)}(\vec{k})\, \mathcal{O}^l(\vec{k}) \cdot \mathcal{O}^l(-\vec{k}) \,, \tag{A3}$$

where

$$\Gamma^{(l)}(\vec{k}) \equiv \sum_{(i-j)} e^{i\vec{k}\cdot(\vec{R}_i - \vec{R}_j)}\, \Gamma^{(l)}(i-j) \,.$$

The operators $\mathcal{O}^l_m(\vec{k})$ of $SU(2s+1)$ satisfy the commutation relations,

$$[\mathcal{O}^l_m(\vec{k}),\, \mathcal{O}^{l'}_{m'}(\vec{k}')] = \frac{1}{\sqrt{N}} \sum_{\substack{l''m'' \\ (l+l'+l''=odd)}} C^{ll'l''}_{mm'm''}\, \mathcal{O}^{l''}_{m''}(\vec{k}+\vec{k}') \,, \tag{A4}$$

where

$$C^{ll'l''}_{mm'm''} = (-)^{2s-m''+1}\, 2([l][l'][l''])^{1/2} \begin{Bmatrix} l & l' & l'' \\ s & s & s \end{Bmatrix} \begin{pmatrix} l & l' & l'' \\ m & m' & -m'' \end{pmatrix}$$

and $[l] \equiv 2l+1$, $\{:::\}$ is a $6-j$ symbol and $(:::)$ is a $3-j$ symbol. The commutator of one of the generators of the group with our Hamiltonian is

$$[\mathcal{O}^{l'}_{m'}(\vec{k}'),\, \mathcal{H}] = \frac{2}{\sqrt{N}} \sum_{\substack{l''m'' \\ (l+l'+l''=odd)}} \sum_{lm} (-)^{m+1} C^{ll'l''}_{mm'm''} \sum_{\vec{k}} \Gamma^{(l)}(\vec{k})\, \mathcal{O}^l_{-m}(\vec{k})\, \mathcal{O}^{l''}_{m''}(\vec{k}'-\vec{k}) \,. \tag{A5}$$

In *general* these commutators of $\mathcal{O}^l_m(\vec{k}=0)$ with $\mathcal{H}$ do not vanish, therefore our $\mathcal{H}$ is not an invariant of the group $SU(2s+1)$, it does not have the maximum symmetry possible in this operator space. However, it may be an invariant of a subgroup of $SU(2s+1)$. We constructed $\mathcal{H}$ so that it is always an invariant of SU(2) or O(3). We can readily show with the commutation relation (A5) that

$$[\mathcal{O}^l_m(0),\, \mathcal{H}] = 0 \text{ or } [s_q,\, \mathcal{H}] = 0$$

and

$$[\mathcal{O}^1(0) \cdot \mathcal{O}^1(0),\, \mathcal{H}] = 0 \text{ or } [s^2,\, \mathcal{H}] = 0 \,, \tag{A6}$$

where $\mathcal{O}^l_m(0) = (1/\sqrt{N})\sum_i \mathcal{O}^l_m(i)$, $s_q \equiv \sum_i s_q(i)$, and $\mathbf{s}^2 = \mathbf{s}\cdot\mathbf{s} = s_x^2 + s_y^2 + s_z^2$. The $\mathcal{O}^l_m(0)$ are the generators of SU(2) and $\mathcal{O}^1(0)\cdot\mathcal{O}^1(0)$ is the bilinear invariant or Casimir operator of SU(2).

Whenever the Hamiltonian for a system has more symmetry than the *spatial* or *geometrical* symmetry of the lattice, we say that the system has *dynamical* symmetry. This additional symmetry comes about because of a special form of the pair interactions between particles or ions. For example, the hydrogen atom $\mathcal{H} = p^2/2m - e^2/r$ has not only O(3) symmetry but also O(4). The degeneracy n^2 of all levels with the same principal quantum number n (different l, m) is explained by the O(4) symmetry. With only O(3) symmetry there would be no reason to have levels with different angular momentum l degenerate.

In our case we consider only interactions with SU(2) or O(3) symmetry, even though our ions are placed on a three-dimensional lattice and realistic interactions between ions are anisotropic. We can contemplate *additional* symmetry whenever the interaction constants $\Gamma^{(l)}(\vec{k})$ assume special relationships among themselves. For example if our range functions $\Gamma^{(l)}(\vec{k})$ are identical for all multipolar interactions, i.e., $\Gamma^{(l)}(\vec{k}) \equiv \Gamma(\vec{k})$ for all l, we find

$$[\mathcal{O}^{l'}_{m'}(0), \mathcal{H}] = 0 \tag{A7}$$

for *all* $l' \leq 2s$ and $-l' \leq m' \leq l'$. Our Hamiltonian $\mathcal{H}$ is similar to the Casimir operator G (bilinear invariant) of SU($2s+1$), i.e.,

$$G[\mathrm{SU}(2s+1)] = \sum_{l=1}^{2s} \mathcal{O}^l \cdot \mathcal{O}^l$$

$$= \sum_{l=1}^{2s} \sum_{i\,j} \mathcal{O}^l(i) \cdot \mathcal{O}^l(j) ,$$

while

$$\mathcal{H} = \sum_{l=1}^{2s} \sum_{i\,j} \Gamma_{ij}\, \mathcal{O}^l(i) \cdot \mathcal{O}^l(j) . \tag{A8}$$

If we take into account that $\Gamma_{ii} = 0$, because there are no interactions on the same site and that the term $\mathcal{O}^l(i)\cdot\mathcal{O}^l(i)$ in G is just a constant, from Eq. (A7) we find that $[G, \mathcal{H}] = 0$. For the Casimir operator the commutator

$$[\mathcal{O}^{l'}_{m'}(\vec{k}'), G] = 0$$

vanishes for all $\vec{k}'$, not only $\vec{k}' = 0$. If we make the additional assumption $\Gamma_{ij} = \Gamma$ our $\mathcal{H}$ to within a constant becomes the Casimir operator G; however, this is not an interesting model because it is equivalent to the molecular-field approximation and does not lead to any dispersion in the excitation spectra. Thus all we can say is that our special Hamiltonian has SU($2s+1$) symmetry for only $\vec{k} = 0$ excitations while the Casimir operator G has this symmetry for all $\vec{k}$.

To label the eigenstates of a Hamiltonian one uses the eigenvalues of operators which commute with $\mathcal{H}$. The only operators which commute with the general Hamiltonian Eq. (A1) are $\mathbf{s}^2$ and s_q, $q = x, y, z$, i.e., $G[\mathrm{SU}(2)]$ and $\mathcal{O}^1_m(0)$. As the $\mathcal{O}^1_m$ do not commute amongst themselves, one chooses only one component and as $\mathcal{H}$ is rotationally invariant, we call it s_z. When $\mathcal{H}$ has some dynamical symmetry there will be more operators which commute with it, e.g., when all $\Gamma^{(l)}$ are equal all $\mathcal{O}^l_m(0)$, $G[\mathrm{SU}(2s+1)]$ and the Casimir operators of the subgroups of SU($2s+1$) commute with $\mathcal{H}$. A *commuting subset* of these operators provides additional labels to specify the $\vec{k} = 0$ eigenstates of our system.

Dynamical symmetry or anisotropy can be observed by noting the degeneracies of $\vec{k} = 0$ levels for the Hamiltonian Eq. (A1), i.e., when special relations exist between the $\Gamma^{(l)}(\vec{k})$ we expect that certain gaps between levels will disappear. There is particular interest in degeneracies (or gaps as the case may be) in the ground and low-lying states of a system, and therefore we focus our attention on the Goldstone theorem. This theorem states that for each symmetry operation of a Hamiltonian, i.e., $[\mathcal{O}^{l'}_{m'}(\vec{k}=0), \mathcal{H}] = 0$ there exists a gapless excitation mode, the Goldstone boson $\mathcal{O}^{l'}_{m'}(\vec{k}=0)$, which acts on the ground state and restores a *continuous* symmetry that has been broken by a phase transition. A system described by Hamiltonian Eq. (A1) has at least *one* Goldstone boson [see Eqs. (A6)], when it has an ordered state which is not rotationally invariant. This boson restores the rotational invariance broken by the ordered phase. When additional dynamical symmetry is present, new Goldstone bosons may exist in low-temperature excitation spectra of ordered systems. These bosons restore the additional symmetry broken by the ordering. Conversely, viewed from the position of a Hamiltonian like (A8) with additional dynamical symmetry, the general Hamiltonian is dynamically anisotropic and instead of a gapless excitation mode, one may find gaps in the spectrum at $\vec{k} = 0$. This corresponds to generators $\mathcal{O}^l_m(0)$ which are no longer symmetry transformations of $\mathcal{H}$. Therefore we can say that *dynamical anisotropy is a possible origin of gaps at* $\vec{k} = 0$ *in some modes of the elementary excitation spectra of systems described by the Hamiltonian, Eq.* (A1).

APPENDIX B: QUALITATIVE FEATURES OF SPECTRA

In this Appendix, we present a qualitative study of the effects of the individual terms in the spin-1 Hamiltonian on the two-spin–deviation spectra,[27]

$$\mathcal{H} = \sum_{\substack{l=1,2 \\ 0 \leq m \leq l}} \mathcal{H}^{(l)}_m , \tag{B1}$$

where

$$\mathcal{H}_m^{(l)} = -\Gamma_m^{(l)}(-1)^m \sum_{i,j} [O_m^l(i)O_{-m}^l(j) + O_{-m}^l(i)O_m^l(j)] , \tag{B2}$$

and $\Gamma_0^{(l)} > 0$. From the commutation relations among the tensor operators O_m^l, Eq. (A4), we find that the z component of the total spin S_z commutes with $O_m^{(l)}$ and hence $\mathcal{H}$, Eq. (B1). That is,

$$[S_z, \mathcal{H}_m^{(l)}] = 0 \tag{B3}$$

for $l = 1$, 2 and $0 \leq m \leq l$. We also see that the z component of the total quadrupole moment Q commutes with $\mathcal{H}_0^{(l)}$ ($l = 1$, 2) and $\mathcal{H}_2^{(2)}$. However, it commutes with $\mathcal{H}_1 \equiv \mathcal{H}_1^{(1)} + \mathcal{H}_1^{(2)}$ only when $\beta_1 \equiv \Gamma_1^{(2)}/\Gamma_1^{(1)} = 1$. That is,

$$\begin{aligned} &[Q, \mathcal{H}_0^{(l)}] = 0 \quad (l = 1, 2) , \\ &[Q, \mathcal{H}_2^{(2)}] = 0 , \end{aligned} \tag{B4}$$

and

$$[Q, \mathcal{H}_1] = 0 \tag{B5}$$

only when $\beta_1 = 1$. Therefore we can always label the eigenstates of $\mathcal{H}$ by the number of spin deviations. It addition, when $\beta_1 = 1$, Q becomes a second label for the eigenstates.

By solving the Schrödinger equation for one-spin-deviation ($m = 1$) states of the system described by $\mathcal{H}$ in Eq. (B1), we find the dispersion relation of spin waves is given as

$$\mathcal{E}(\vec{k}) = z(\Gamma_0^{(1)} + \Gamma_0^{(2)}) - (\Gamma_1^{(1)} + \Gamma_1^{(2)}) \sum_{\vec{\delta}} \cos(\vec{k} \cdot \vec{\delta}) . \tag{B6}$$

We note that the dispersion in the spectra results from $\mathcal{H}_1$ which contains the terms proportional to $s_i^+ s_j^-$. $\mathcal{H}_2^{(2)}$ has no effect on $m = 1$ states.

To see the effects of the individual terms $\mathcal{H}_m^{(l)}$ on the two-spin-deviation spectra, we start from the Ising term, $\mathcal{H}_0 \equiv \mathcal{H}_0^{(1)} + \mathcal{H}_0^{(2)}$. The energy spectrum is shown in Fig. 11(a). The thick solid line represents the quadrupolar (single-ion $m = 2$) excitations, whose energies are given as

$$\mathcal{E}_1 = 2z\Gamma_0^{(1)} , \tag{B7}$$

and whose amplitudes behave as $\delta(\vec{R}, 0)$, where $\vec{R}$ is the separation between two ions on which the two spin-deviations occur. This energy level is N-fold degenerate, where N is the number of ions in the lattice. The thin solid line represents N neighboring-ion excitations whose energies are given as

$$\mathcal{E}_2 = (2z - 1)\Gamma_0^{(1)} + (2z - 3)\Gamma_0^{(2)} , \tag{B8}$$

and whose amplitudes behave as $\delta(\vec{R}, \vec{\delta})$, where $\vec{\delta}$ is the vector connecting nearest-neighbor ions. The dashed line represents the $\frac{1}{2}N(N-3)$ non-neighboring-ion excitations, whose energies are

$$\mathcal{E}_3 = 2z(\Gamma_0^{(1)} + \Gamma_0^{(2)}) , \tag{B9}$$

and whose amplitudes behave as $1 - \delta(\vec{R}, 0) - \delta(\vec{R}, \vec{\delta})$.

The terms in $\mathcal{H}_2^{(2)}$ are proportional to $(s_i^+)^2$ $(s_j^-)^2$, and they propagate quadrupolar (single-ion $m = 2$) excitations through the lattice. Therefore $\mathcal{H}_2^{(2)}$ produces a dispersion in the energy spectra for the quadrupolar excitations of $\mathcal{H}_0$. In the system described by $\mathcal{H}_0 + \mathcal{H}_2^{(2)}$, the dispersion relation for the quadrupole waves with wave vector $\vec{K}$,

$$|\psi(\vec{K})\rangle = \sum_i e^{i\vec{K}\cdot\vec{r}_i}(s_i^-)^2|g\rangle = 2\sum_i e^{i\vec{K}\cdot\vec{r}_i} O_{-2}^2(i)|g\rangle , \tag{B10}$$

is given as

$$\mathcal{E}(\vec{K}) = 2\left(z\Gamma_0^{(1)} - \Gamma_2^{(2)} \sum_{\vec{\delta}} \cos(\vec{K} \cdot \vec{\delta})\right) . \tag{B11}$$

This dispersion curve is shown by the thick solid line in Fig. 11(b). The two-ion excitations are not affected by the presence of $\mathcal{H}_2^{(2)}$ because

$$\mathcal{H}_2^{(2)} \sum_{i \neq j} \phi(i, j) s_i^- s_j^- |g\rangle = 0 . \tag{B12}$$

The effect of $\mathcal{H}_1$ on the spectra can be seen by dividing it into two parts,

$$\begin{aligned} \mathcal{H}_1' &\equiv \mathcal{H}_1^{(1)} + \mathcal{H}_1^{(2)}/\beta_1 \\ &= -\Gamma_1^{(1)} \sum_{l=1,2} \sum_{i,j} [O_1^l(i)O_{-1}^l(j) + O_{-1}^l(i)O_1^l(j)] \end{aligned}$$

and

$$\begin{aligned} \mathcal{H}_1'' &\equiv (1 - 1/\beta_1)\mathcal{H}_1^{(2)} \\ &= -(\Gamma_1^{(2)} - \Gamma_1^{(1)}) [O_1^2(i)O_{-1}^2(j) + O_{-1}^2(i)O_1^2(j)] . \end{aligned} \tag{B13}$$

We note that

$$\mathcal{H}_1' = \mathcal{H}_1 \text{ when } \beta_1 = 1 . \tag{B14}$$

Therefore, from Eq. (B5), we see that $\mathcal{H}_1'$ conserves Q and hence does not mix two-ion excitations with quadrupole waves. However, $\mathcal{H}_1'$ consists of terms of the type $s_i^+ s_j^-$, and it mixes neighboring and non-neighboring-ion excitations. Again, using the commutation relations of O_m^l, we find that

$$[\mathcal{H}_1', O_{-2}^2(\vec{K})]|g\rangle = 0 . \tag{B15}$$

This relation implies that $\mathcal{H}_1'$ does not affect the dispersion relation of quadrupole waves, Eq. (B11). However, it does affect the two-ion excitation spectra as shown in Figs. 12(a) and 12(b) for two different sets of the pair coupling parameters, $\Gamma_m^{(l)}$. The cross-hatched areas in the figure represent two-spin-wave bands and the thin solid lines represent exchange bound states. The quadrupole wave dispersion curves are represented by the thick solid lines. We note in Fig. 12(a), that the energies of the quadrupole waves overlap with the two-spin-wave band.

When we further include $\mathcal{H}_1''$, Q is no longer a

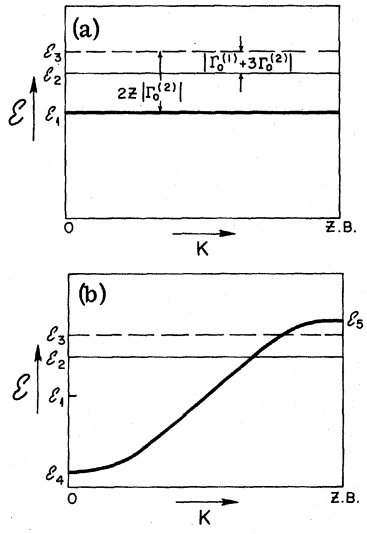

FIG. 11. (a) Two-spin–deviation spectra for $\mathcal{H}_0 \equiv \mathcal{H}_0^{(1)} + \mathcal{H}_0^{(2)}$. The thick solid line represents the quadrupolar (single-ion $m=2$) excitations whose energies are given as $\mathcal{E}_1 = 2z\Gamma_0^{(1)}$. The thin solid line represents the neighboring-ion excitations with energy $\mathcal{E}_2 = (2z-1)\Gamma_0^{(1)} + (2z-3)\Gamma_0^{(2)}$. The dashed line represents the non-neighboring-ion excitations with energy $\mathcal{E}_3 = 2z(\Gamma_0^{(1)} + \Gamma_0^{(2)})$. (b) The two-spin–deviation spectra for $\mathcal{H}_0 + \mathcal{H}_2^{(2)}$. The thick solid line represents the dispersion curve for quadrupole waves, Eq. (B11). $\mathcal{E}_4 = 2z(\Gamma_0^{(1)} - \Gamma_2^{(2)})$, and $\mathcal{E}_5 = 2z(\Gamma_0^{(1)} + \Gamma_2^{(2)})$. Note that the thin solid line and dashed line are the same as in 11 (a).

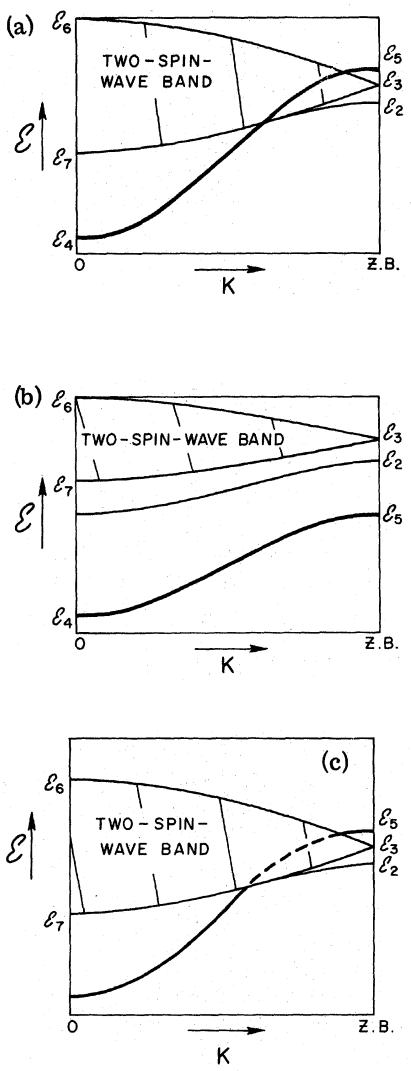

FIG. 12. (a) Two-spin–deviation spectra for $\mathcal{H}_0 + \mathcal{H}_2^{(2)} + \mathcal{H}_1^{\prime}$. The cross-hatched area represents the two-spin-wave band. $\mathcal{E}_6 = \mathcal{E}_3 + 2z|\Gamma_1^{(1)} + \Gamma_1^{(2)}|$ and $\mathcal{E}_7 = \mathcal{E}_3 - 2z|\Gamma_1^{(1)} + \Gamma_1^{(2)}|$. The thin solid line below the band represents the two-spin-wave bound states, which have energy $\mathcal{E}_2$ at the zone boundary. The fraction of the Brillouin zone in which the bound states exist depends on the relative magnitudes of the exchange parameters $\Gamma_m^{(1)}$. The thick solid line represents the quadrupole waves. (b) The same case as 12(a), except for a different set of exchange parameters $\Gamma_m^{(1)}$. (c) The two-spin–deviation spectra for $\mathcal{H}$ for $\beta_1 \sim 1$. The broken line in the band represents the energies of the quadrupolar resonant states. The thick solid line outside the band which connects to the broken line represents the single-ion bound states. The thin solid line below the band represents the exchange bound states.

good quantum number of the system. Therefore, the quadrupole waves become single-ion bound states outside the band[23] and quadrupolar resonant states within the band. The lifetime of these quadrupolar resonant states decreases as $|\beta_1 - 1|$ increases and the energy of the resonant states is shifted from the quadrupole wave energy by an amount which increases with $|\beta_1 - 1|$. Furthermore, the exchange bound states gain a finite amplitude for two spin-deviations at zero separation. In Fig. 12(c), we show the spectra for $\beta_1 \sim 1$. The broken line in the band shows the energy of the quadrupolar resonant states. The thick solid line outside the band which connects to the broken line represents the single-ion bound states.[23] In the case of Fig. 12(b), the dispersion curve of the quadrupole waves lies completely outside the band. Then the inclusion of $\mathcal{H}_1^{\prime}$ only leads to single-ion bound states.[3]

The above qualitative features are the same for lattices of all dimensions, although the quantitative aspects do depend on lattice structure.

APPENDIX C: SYMMETRY OF BOUND-STATE WAVE FUNCTIONS

In this Appendix, we study the symmetry of the wave functions of two-spin-wave bound states for the simple-cubic lattice. From Eqs. (26a), (27), and (28), we see that the bound state wave functions are given as

$$\varphi_{\vec{K}}(\vec{R})=\frac{1}{N}\sum_{\rho_1\rho_2\rho_3}\frac{\cos(\vec{\rho}\cdot\vec{R})[A_0+2\sum_{i=1,2,3}A_i\cos(\rho_i a)]}{2z\Gamma^{(1)}(1+\beta)[t-\alpha\sum_{i=1,2,3}\cos(\rho_i a)/3]}, \tag{C1}$$

where t satisfies Eq. (56a) or (56b) if the total wave vector $\vec{K}$ is along the cube diagonal, i.e., $\vec{K}=K(1,\ 1,\ 1)$ and $\vec{\rho}\equiv(\rho_1, \rho_2, \rho_3)$. By substituting Eq. (56a) into Eq. (52), we find that

$$A_0+2\alpha(A_1+A_2+A_3)=0\ ,$$

and

$$M_{10}A_0+M_{12}(A_1+A_2+A_3)=0\ . \tag{C2}$$

Since $M_{12}-2\alpha M_{10}\neq 0$ unless Eq. (56b) is also satisfied, Eq. (C2) has only trivial solutions. That is, $A_0=0$ and $A_1+A_2+A_3=0$. Therefore, the wave function Eq. (C1) is written as

$$\varphi_K(x, y, z)=\frac{1}{N}\sum_{\rho_1\rho_2\rho_3}\frac{\cos(\rho_1 x+\rho_2 y+\rho_3 z)\sum_{i=1,2}A_i[\cos(\rho_i a)-\cos(\rho_3 a)]}{z\Gamma^{(1)}(1+\beta)[t-\alpha\sum_{i=1,2,3}\cos(\rho_i a)/3]}\ . \tag{C3}$$

This function has d symmetry in coordinate space.

By substituting Eq. (56b) into Eq. (52), we obtain

$$\begin{bmatrix} 1 & 2\alpha & 2\alpha & 2\alpha \\ M_{10} & 6\alpha M_{10}-2M_{12} & M_{12} & M_{12} \\ M_{10} & M_{12} & 6\alpha M_{10}-2M_{12} & M_{12} \\ M_{10} & M_{12} & M_{12} & 6\alpha M_{10}-2M_{12} \end{bmatrix}\begin{bmatrix} A_0 \\ A_1 \\ A_2 \\ A_3 \end{bmatrix}=0\ . \tag{C4}$$

This equation is satisfied if

$$A_1=A_2=A_3=A$$

and

$$A_0=-6\alpha A\ . \tag{C5}$$

Therefore, the wave function Eq. (C1) is given as

$$\varphi_K(x, y, z)=\frac{A}{N}\sum_{\rho_1\rho_2\rho_3}\frac{\cos(\rho_1 x+\rho_2 y+\rho_3 z)[\sum_{i=1,2,3}\cos(\rho_i a)-3\alpha]}{z\Gamma^{(1)}(1+\beta)[t-\alpha\sum_{i=1,2,3}\cos(\rho_i a)/3]}\ . \tag{C6}$$

This function has s symmetry in coordinate space.

---

*Research supported in part by the National Science Foundation under Grants No. DMR72-02947 and GU3186.

[1]W. P. Wolf, J. Phys. (Paris) 32, C1-26 (1971); J. M. Baker, Rep. Prog. Phys. 34, 109 (1971); P. M. Levy, in *Magnetic Oxides*, edited by D. J. Craik (Wiley, London, 1975), Chap. 4.

[2]D. A. Pink and P. Tremblay, Can. J. Phys. 50, 1728 (1972).

[3]D. A. Pink and R. Ballard, Can. J. Phys. 52, 33 (1974).

[4]B. Westwański, Phys. Lett. A 44, 27 (1973), and unpublished. We thank Dr. Westwański for sending us preprints of his work.

[5]J. Sivardière, Int. J. Mag. (to be published). We thank Dr. Sivardière for sending us preprints of his work.

[6]M. Nauciel-Bloch, G. Sarma, and A. Castets [Phys. Rev. B 5, 4603 (1972)], D. A. Pink and R. Ballard [Ref. 3], M. Barma [Phys. Rev. B 10, 4650 (1974), and Y. Y. Hsieh (private communication) have given conditions on the interaction parameters to assure a ferromagnetic ground state.

[7]B. R. Judd, *Operator Techniques in Atomic Spectroscopy* (McGraw-Hill, New York, 1963).

[8]T. Moriya, J. Phys. Soc. Jpn. 29, 117 (1970).

[9]R. J. Elliott and R. Loudon, Phys. Lett. 3, 189 (1963).

[10]M. F. Thorpe, Phys. Rev. B 4, 1608 (1971).

[11]D. Kim and R. I. Joseph [Phys. Lett. A 44, 75 (1973)] have found the excitation spectrum for the Schrödinger Hamiltonian ($\beta=1$) from the quadrupolar ground state. We find that both the spin-wave and quadrupole-wave excitations from the ferromagnetic ground state, which is degenerate with the quadrupolar ground state for $\beta=1$, have the same dispersion relations as that found by Kim and Joseph.

[12]R. Silberglitt and J. B. Torrance, Jr., Phys. Rev. B 2, 772 (1970).

[13]R. Silberglitt and A. B. Harris, Phys. Rev. Lett. 19, 30 (1967); Phys. Rev. 174, 640 (1968); R. Silberglitt, Ph.D. thesis (University of Pennsylvania, 1968) (unpublished).

[14]M. Wortis, Phys. Rev. 132, 85 (1963).

[15]J. Hanus, Phys. Rev. Lett. 11, 336 (1963).

[16]S. T. Chiu-Tsao, Phys. Rev. B 4, 3098 (1971).

[17]I. Mannari and C. Kawabata, Research Notes of Physics Department, Okayama University, No. 15, 1964 (unpublished).

[18]A. A. Maradudin, E. W. Montroll, G. H. Weiss, R. Herman, and H. W. Milnes, Acad. Roy. Belgique,

Memoires, XIV, No. 1709 (1960). We thank Dr. C. H. Wu for bringing this reference and Ref. 20 to our attention.

[19]M. Wortis, Ph.D. thesis (Harvard University, 1963) (unpublished).

[20]E. M. Baroody, J. Math. Phys. 10, 475 (1969).

[21]These Van Hove singularities were shown in Fig. 1 of Ref. 10. Owing to an algebraic mistake the density of states for $\beta = 0$ given in that paper is incorrect. We thank Prof. Thorpe for a discussion of this point. A. M. Bonnot and J. Hanus, Phys. Rev. B 7, 2207 (1973).

[22]Admittedly, this is a rather difficult experimental determination.

[23]D. A. Pink and R. Ballard (Ref. 3) have discussed the presence of single-ion bound states outside the two-spin-wave band for this case. Here we are pointing out that quadrupolar resonant states exist inside the band.

[24]R. J. Elliott, R. T. Harley, W. Hayes, and S. R. P. Smith, Proc. R. Soc. A 328, 217 (1972).

[25]J. K. Kjems, G. Shirane, R. J. Birgeneau, and L. G. Van Uitert, Phys. Rev. Lett. 31, 1300 (1973); R. T. Harley, W. Hayes, A. M. Perry, and S. R. P. Smith, J. Phys. C 6, 2382 (1973).

[26]G. Dolling and R. A. Cowley, Phys. Rev. Lett. 16, 683 (1966); R. J. Elliott *et al.*, Ref. 24; G. A. Gehring and K. A. Gehring, Rep. Prog. Phys. 38, 1 (1975).

[27]To the best of our knowledge, this approach of studying the qualitative features of two-spin–deviation spectra was first used by J. B. Torrance, Jr., and subsequently by R. Silberglitt and A. B. Harris [Comments Solid State Physics 2, 8 (1970)].